PB82-102328

# FEASIBILITY OF BURNING COAL IN CATALYTIC COMBUSTORS

P. M. Goldberg, et al

Acurex Corporation
Mountain View, CA

U.S. Department of Commerce
National Technical Information Service
NTIS

PB82-102328

EPA-600/7-81-150

# FEASIBILITY OF BURNING COAL IN CATALYTIC COMBUSTORS

by

P.M. Goldberg, E.K. Chu, and J.T. Kelly

Acurex Corporation
485 Clyde Avenue
Mountain View, California 94042

Contract No. 68-02-2611, Task 30

EPA Project Officer: G. Blair Martin

Industrial Environmental Research Laboratory
Office of Environmental Engineering and Technology
Research Triangle Park, North Carolina 27711

Prepared for

U.S. Environmental Protection Agency
Office of Research and Development
Washington, D.C. 20460

REPRODUCED BY
NATIONAL TECHNICAL
INFORMATION SERVICE
U.S. DEPARTMENT OF COMMERCE
SPRINGFIELD, VA. 22161

IERL-RTP-1248

**TECHNICAL REPORT DATA**
*(Please read Instructions on the reverse before completing)*

| 1. REPORT NO. | 2. | 3. RECIPIENT'S ACCESSION NO. PB82 102328 |
|---|---|---|
| 4. TITLE AND SUBTITLE<br>Feasibility of Coal Burning in Catalytic Combustors | | 5. REPORT DATE<br>6. PERFORMING ORGANIZATION CODE |
| 7. AUTHOR(S)<br>P. M. Goldberg, E. K. Chu, and J. T. Kelly | | 8. PERFORMING ORGANIZATION REPORT NO. |
| 9. PERFORMING ORGANIZATION NAME AND ADDRESS<br>Acurex Corporation<br>Energy and Environmental Division<br>485 Clyde Avenue<br>Mountain View, California 94042 | | 10. PROGRAM ELEMENT NO.<br>11. CONTRACT/GRANT NO.<br>68-02-2611, Task 30 |
| 12. SPONSORING AGENCY NAME AND ADDRESS<br>EPA, Office of Research and Development<br>Industrial Environmental Research Laboratory<br>Research Triangle Park, NC 27711 | | 13. TYPE OF REPORT AND PERIOD COVERED<br>Task Final; 5/78-11/78<br>14. SPONSORING AGENCY CODE<br>EPA/600/13 |

15. SUPPLEMENTARY NOTES IERL-RTP project officer is G. Blair Martin, Mail Drop 62, 919/541-7504.

16. ABSTRACT The report gives results of a study, showing that pulverized coal can be burned in a catalytic combustor. Pulverized coal combustion in catalytic beds is markedly different from gaseous fuel combustion. Gas combustion gives uniform bed temperatures and reaction rates over the entire bed length; however, depending on flow conditions and bed geometry, little combustion may occur downstream of the bed. For the bed configurations, fuel supplies, and test conditions studied, pulverized coal combustion results in significant temperature and reaction gradients over the bed length and substantial combustion downstream of the bed. Thus, for pulverized coal combustion, the bed acts mainly as a combustion initiator and stabilizer. A significant portion of the combustion process, primarily that associated with char burnout, occurs downstream of the bed.

17. KEY WORDS AND DOCUMENT ANALYSIS

| a. DESCRIPTORS | b. IDENTIFIERS/OPEN ENDED TERMS | c. COSATI Field/Group |
|---|---|---|
| Pollution<br>Pulverized Fuels<br>Coal<br>Combustion<br>Catalysis | Pollution Control<br>Stationary Sources<br>Catalytic Combustion | 13B<br>21D<br><br>21B<br>07D |

| 18. DISTRIBUTION STATEMENT | 19. SECURITY CLASS (This Report) | 21. |
|---|---|---|
| Release to Public | Unclassified | |
| | 20. SECURITY CLASS (This page) Unclassified | 22. PRICE |

EPA Form 2220-1 (9-73)

NOTICE

THIS DOCUMENT HAS BEEN REPRODUCED FROM THE BEST COPY FURNISHED US BY THE SPONSORING AGENCY. ALTHOUGH IT IS RECOGNIZED THAT CERTAIN PORTIONS ARE ILLEGIBLE, IT IS BEING RELEASED IN THE INTEREST OF MAKING AVAILABLE AS MUCH INFORMATION AS POSSIBLE.

## DISCLAIMER

This report has been reviewed by the Industrial Environmental Research Laboratory (RTP), U.S. Environmental Protection Agency, and approved for publication. Approval does not signify that the contents necessarily reflect the views and policies of the Agency, nor does mention of trade names or commercial products constitute endorsement or recommendation for use.

TABLE OF CONTENTS


| Section | | Page |
|---|---|---|
| 1 | INTRODUCTION | 1 |
| 2 | CATALYTIC COAL COMBUSTOR MODEL | 2 |
| | 2.1 Operating Characteristics and Assumptions | 2 |
| | 2.2 Governing Equations | 4 |
| | 2.3 Model Solutions | 7 |
| | 2.4 Conclusions | 17 |
| 3 | FEASIBILITY TESTING | 21 |
| | 3.1 Experimental Equipment | 21 |
| | 3.1.1 Catalyst Housing | 21 |
| | 3.1.2 Catalyst Beds | 24 |
| | 3.1.3 Sampling System | 24 |
| | 3.1.4 Coal Feed System | 27 |
| | 3.1.5 Temperature and Pressure Monitoring | 27 |
| | 3.2 Feasibility Test Results | 28 |
| | 3.2.1 Test Series 1 | 28 |
| | 3.2.2 Test Series 2 | 29 |
| | 3.2.3 Test Series 3 | 32 |
| | 3.2.4 Test Series 4 | 36 |
| | 3.3 Test Results | 37 |
| | 3.3.1 Bed Temperature | 41 |
| | 3.3.2 Bed Pressure | 45 |
| | 3.3.3 Extent of Reaction | 48 |
| | 3.3.4 Emissions | 50 |
| | 3.4 Summary | 53 |
| 4 | EVALUATION TESTING | 54 |
| | 4.1 Experimental Equipment | 54 |
| | 4.1.1 Catalytic Bed | 56 |
| | 4.1.2 Sampling System | 56 |
| | 4.1.3 Temperature Monitoring | 56 |
| | 4.1.4 Coal and Feed System | 60 |

TABLE OF CONTENTS -- Concluded


| Section | | Page |
|---|---|---|
| | 4.2 Test Results . . . . . | 60 |
| | 4.2.1 Test Procedures . . . . . | 60 |
| | 4.2.2 Operating Characteristics . . . . . | 61 |
| | 4.2.3 Test Data . . . . . | 67 |
| | 4.2.4 Comparison with Conventional Combustion . . . . | 77 |
| 5 | CONCLUSIONS AND RECOMMENDATIONS . . . . . | 81 |
| | REFERENCES . . . . . | 84 |

LIST OF ILLUSTRATIONS


| Figure | | Page |
|---|---|---|
| 1 | Coal-Fired Catalytic Combustor Model Schematic . . . . | 2 |
| 2 | Constant Coal Flow Combustor Length Map for 70 Micron Particles . . . . . | 8 |
| 3 | Minimum Bed Length and Temperatures for Stable Operation for Various Air/Fuel Ratios . . . . . | 10 |
| 4 | Temperature, Volatilization and Particle Mass Histories Along Bed . . . . . | 12 |
| 5 | Constant Airflow Combustor Length Map for 70 Micron Particles . . . . . | 14 |
| 6 | Mininum Bed Length Particle, Gas, and Bed Exit Temperatures for Various Air/Fuel Ratios . . . . . | 15 |
| 7 | Minimum Bed Length Percent Volatilization, Particle and Oxygen Mass Left at Combustor Exit . . . . . | 16 |
| 8 | Constant Airflow Combustor Length Map for 25 Micron Particles . . . . . | 18 |
| 9 | Constant High Airflow Combustor Length Map for 25 Micron Particles . . . . . | 19 |
| 10 | Combustion System Flow Diagram . . . . . | 22 |
| 11 | Catalyst Housing . . . . . | 23 |
| 12 | Sampling System Flow . . . . . | 25 |
| 13 | Bed and Gas Temperatures -- Test Series 1 . . . . . | 30 |
| 14 | Post-test View of Test Series 1 Catalyst Bed . . . . . | 31 |
| 15 | Post-test View of Test Series 3 Catalyst Bed . . . . . | 35 |
| 16 | Post-test View of Test Series 4 Catalyst Bed . . . . . | 38 |
| 17 | Variation of Combustor Temperatures with Time . . . . . | 42 |
| 18 | Combustor Temperature and Pressure Variations with Time . . . . . | 43 |
| 19 | Variations of Combustor Temperatures with Time . . . . | 44 |

LIST OF ILLUSTRATIONS (Concluded)


| Figure | | Page |
|---|---|---|
| 20 | Prebed Chamber Pressure During Test Series 4 . . . . . | 46 |
| 21 | Fraction of Channels Open During Test Series 45 . . . . | 47 |
| 22 | Extent of Reaction Versus Air/Fuel Ratio for Feasibility Tests . . . . . | 49 |
| 23 | Exit NO Concentrations for Various Air/Fuel Ratios . . | 51 |
| 24 | Exit NO Concentrations Versus Extent of Coal Reaction . | 52 |
| 25 | Catalytic Coal Combustion Test Section . . . . . | 55 |
| 26 | Assembled Catalytic Coal Test System . . . . . | 57 |
| 27 | Bed Thermocouple Locations . . . . . | 59 |
| 28 | Typical Bed and Gas Temperature Distributions During Coal Combustion . . . . . | 62 |
| 29 | Comparison of Measured and Predicted Bed Temperatures . . . . . | 64 |
| 30 | Bed Temperature Distributions when Operating with Propane . . . . . | 65 |
| 31 | Extent of Coal Reaction with Air/Fuel Ratio . . . . . | 70 |
| 32 | SEM Photomicrographs of Unreacted and Reacted Utah Coal Samples . . . . . | 71 |
| 33 | Bed Temperature Variation with Air/Fuel Ratio . . . . . | 73 |
| 34 | Measured Exit NO Variation with Air/Fuel Ratio . . . . | 76 |
| 35 | Measured Exit NO Variation with Bed Temperature . . . . | 78 |

LIST OF TABLES


| Table | | Page |
|---|---|---|
| 1 | Coal Characteristics . . . . . | 9 |
| 2 | Analytical Equipment Used . . . . . | 26 |
| 3 | Feasibility Test Data Summary . . . . . | 39 |
| 4 | Monolith Catalyst Coatings . . . . . | 58 |
| 5 | Evaluation Test Data Summary . . . . . | 68 |

# SECTION 1

# INTRODUCTION

Catalytic combustion of clean gaseous fuels and light oils has shown considerable promise as a means of reducing emissions and increasing combustion stability and uniformity (Reference 1). Recent catalytic combustor tests with heavy oils with significant bound nitrogen content indicate that, with proper combustor design, the same desirable combustion qualities can also be achieved with these fuels. The combustion of pulverized coal in a catalytic monolith might also offer similar advantages. However, significant differences exist between liquid fuels and solid coal which can lead to additional operational problems. For example, coal contains significant ash which can impact and adhere to combustor surfaces. Also, when heated, the coal goes through a plastic state in which it can adhere to other coal particles or combustor surfaces, altering flow patterns and possibly blocking passages within the combustor. Even if the particles do not stick to the combustor surface, their impact might erode the combustor surface, leading to changes in combustion characteristics or even failure of the combustor. Besides these problems, coal has a volatilization and heterogeneous burnout history which is distinct from oil combustion, requires high temperatures and which may not easily lend itself to catalytic combustion.

Given these problems, the purpose of this study was to determine the feasibility and to evaluate the benefits, if any, of burning pulverized coal in a catalytic combustor. The study consisted of a three-phase effort. In the first phase, existing experimental data on coal heating, volatilization and oxidation rates were used in a simple mathematical model to define combustor configurations and operating regions which had the greatest potential for success. In the second phase, an experimental combustor was constructed based on the results of Phase I, and preliminary tests were run to establish feasible operating regions. Given that feasible regions could be attained, the final phase of the program evaluated the catalytic combustion of coal on the basis of combustion, emission and lifetime characteristics.

The following sections of this report discuss the three program phases. These sections are followed by a conclusions and recommendations section.

## SECTION 2

## CATALYTIC COAL COMBUSTOR MODEL

A simple mathematical model of a coal-fired catalytic combustor was developed to help define combustor configurations and operating regions which have the greatest potential for success. The results of these calculations were also used as an aid in interpreting experimental results. The calculations focused on the combustion and heat transfer aspects of the system. Emissions performance was not included in the calculations.

### 2.1 OPERATING CHARACTERISTICS AND ASSUMPTIONS

The model of the coal-fired catalytic combustor is depicted in Figure 1. The prebed chamber is a large diameter cylindrical tube and the catalytic combustor is a ceramic cylinder of the same diameter in which many small diameter cylindrical passages are formed. A mixture of uniformly distributed monosized coal particles and air enters the prebed chamber at the top of the schematic. This is a steady-state model which assumes the bed is already hot and conditions are constant in time. The velocity of the coal particles is assumed to be the same as the gas velocity, i.e., no particle lags. While in the prebed chamber, the coal

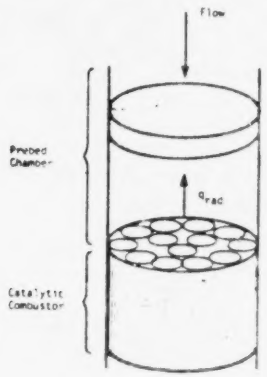


Figure 1. Coal-fired catalytic combustor model schematic.

particles are heated through conduction heat transfer from the preheated air and radiative heat transfer emitted from the front of the combustor. The heated coal then begins to devolatilize to an extent which is dependent on temperature. In the model, combustion of the coal or volatiles is not allowed to occur in the prebed section. This is reasonable since, in a real combustor, operating conditions would be sought for which prebed combustion did not occur. All the results presented are for conditions at which the prebed section cannot possibly sustain combustion by virtue of its low temperature and high velocity.

Upon entering the catalytic combustor, the coal and air mixture is strongly heated by radiation from the hot catalytic combustor surface. The combustor consists of a ceramic cylinder in which many small* diameter catalytically coated channels are formed. Because of the small diameter of the channels the bulk of the particles are in close proximity to catalytically coated walls. Thus radiation exchange occurs freely between the particles and the channel walls. Also, coal volatiles released either in the prebed chamber or within the combustor, will combust in the vicinity of the particle or diffuse to the surface and combust, releasing heat which maintains high catalytic combustor surface temperatures.

Several assumptions are used in the catalytic combustor part of the model to simplify the solution procedure. A major assumption is that the bed temperature is held constant over the combustor length. This is the infinite bed conduction or the uniform surface reactivity no bed heat loss case. This condition is approached by some premixed gas combustor test results (Reference 1) and on that basis may be justified. However, coal is an evolving fuel source and a uniform distribution of surface reaction along the channel length may not be justified. Another major assumption in the model is that all of the volatile combustion occurs on the surface. This is probably justified only up to the local ignition point of the volatiles which has been estimated to be on the order of 1000 K (Reference 2). Once the gas temperature in the vicinity of the particle is above this value, local burning of the volatiles probably takes place. This would result in a more rapid consumption of fuel than that predicted on the basis of diffusion transport to and combustion at the walls. Hence, predictions of the simplified model represent conservative estimates of the degree of combustion. A third assumption is that the surface reactions are in equilibrium and all volatiles reaching the walls of the catalytic combustor will be consumed. This is probably an overall fair assumption if bed temperature is high and small deviations from this behavior are ignored. In conclusion, several assumptions simplify the model solution procedure. However, these assumptions also limit the accuracy of the model.

The governing equations and empirical rate equations used in the model are presented below.

---

*Small with respect to prebed section diameter but very large compared to coal particle size.

## 2.2 GOVERNING EQUATIONS

In the prebed chamber, the energy balance equation for coal particles is given by:

$$\dot{m}_p C_{p_p} dT_p - A\, dq_r + h_p (T_p - T_g)\, dA_p = 0 \qquad (1)$$

where

$\dot{m}_p$ = mass flowrate of coal particles

$C_{p_p}$ = specific heat of coal particles

$T_p$ = coal particle temperature

$A$ = cross sectional area of the prebed chamber

$dq_r$ = thermal radiation from the frontal surface of the catalytic combustor deposited over distance dx

$h_p$ = film heat transfer coefficient for coal particles and air

$T_g$ = gas temperature

$dA_p$ = total surface area of coal particles in an infinitesimal distance dx

The radiative heat transfer from the combustor to location x, measured from the end of the prebed section, is determined by Lambert's attenuation law (Reference 3).

$$q_r(x) = \varepsilon_s \sigma T_s^4 \exp - \kappa (x_o - x) \qquad (2)$$

where

$\varepsilon_s$ = combustor emissivity

$T_s$ = combustor bed temperature

$\kappa$ = absorption coefficient

$x_o$ = total length of the prebed chamber

$\sigma$ = Stefan Boltzmann constant

The absorption coefficient, $\kappa$, is defined as the total projected area of coal particles in a unit volume, and is given by:

$$\kappa = na \qquad (3)$$

where

n = number density of coal particles

a = projected area

The film heat transfer coefficient, $h_p$, is determined by using the approximation for small Reynold's number, i.e.,

$$Nu = \frac{h_p \, d_p}{k} = 2.0 \tag{4}$$

where

$d_p$ is the coal particle diameter and k is the thermal conductivity of the gas.

The energy balance equation for gas is given by:

$$\dot{m}_g \, C_{p_g} \, d \, T_g - h_p \, (T_p - T_g) \, d \, A_p = 0 \tag{5}$$

where

$\dot{m}_g$ = total mass flowrate of gas

$C_{p_g}$ = specific heat of gas

Gas is assumed to be transparent with respect to the radiation emitted from the combustor.

The pyrolysis kinetics of the coal particles used in the model is a simple one-step Arrhenius-type rate expression obtained from Reference 4. It is written as follows:

$$\frac{dV}{dt} = 6.6 \times 10^4 \exp \, (100 - V) \left[-25{,}000/RT_p\right] \tag{6}$$

where

V = percent volatilization of coal particle

R = Universal gas constant

t = time

Considering the variability of coal supplies and the scatter of volatilization data, this simple model was considered adequate for the purpose of assessment of operating regions.

Within the catalytic combustor, heat transfer between coal particles and gas and between coal particles and the hot catalytic surface is included in the model. Also, the heat generation resulting from heterogeneous combustion of the coal particle is accounted for in the model. As indicated previously, coal volatiles combustion is assumed to occur only at the catalyst surface. The equation describing these phenomena is:

$$\dot{m}_p C_{p_p} dT_p + \quad p \quad (T_p^4 - T_s^4)\, d A_p + h_p (T_p - T_g)\, d A_p - \dot{m}_c'' \quad H_c\, d A_p = 0 \qquad (7)$$

where $\dot{m}_c''$ is the carbon surface oxidation kinetic rate and $H_c$ is the heat of combustion corresponding to the surface reaction. The expression for the coal oxidation rate, $m_c''$, was obtained from Reference 5, and is given by:

$$\dot{m}_c'' = 8710 \exp\,(-35{,}700/RT_p)\, P_{O_2} \quad gm/cm^2 sec \qquad (8)$$

where R is the universal gas constant and $P_{O_2}$ is the partial pressure of oxygen. As with the volatilization model, a simple model was felt to be adequate for the purpose of the program.

The energy balance equation of air and the combustion products within the catalytic combustor is given by:

$$\dot{m}_g C_{p_g} dT_g - h_p (T_p - T_g)\, dA_p + h_c N_c C_c (T_g - T_s) dx + C_{p_v} (T_g - T_p)\, d\dot{m}_v = 0 \qquad (9)$$

where

$h_c$ = the film heat transfer coefficient between the hot catalytic surface and the gas, and is determined by

$$Nu = 3.66 = \frac{hd}{k}$$

$N_c$ = number of catalytic channels in the combustor

$C_c$ = circumference of a catalytic channel

The total energy released at the surface at any given distance along the combustor is given by the diffusion-controlled volatiles combustion expression:

$$dQ = C_m N_c C_c\, dx\, Y_v H_{cv} \qquad (10)$$

where $C_m$ is the mass transfer coefficient, $Y_v$ the volatile mass fraction in the stream and $H_{cv}$ the heat of combustion of the volatiles.

Numerical solution of Equations (1), (5), (7), (9), and (10) under the constraint of overall adiabatic conditions in the bed defines the stable operating conditions for a combustor of a given length, channel geometry and initial input conditions. These solutions are discussed in the following sections.

## 2.3 MODEL SOLUTIONS

Figure 2 gives the calculated bed temperatures achieved by combustors of various lengths for a fixed coal feed rate and particle size. Coal properties and particle size distributions for the coals used in this study are given in Table 1. Each separate curve on Figure 2 corresponds to a different air/fuel ratio and the curves span the complete range from fuel-rich to lean conditions. The stoichiometric air/fuel ratio for the Utah coal burned in the bulk of this study was approximately 9. The air preheat temperature utilized in these calculations corresponds to the maximum available from the experimental system. It was felt that a high preheat would represent a good starting condition since initiation of volatilization processes requires fairly high temperatures (Reference 4). A channel diameter of 0.635 cm was chosen for the calculations because it represents a good compromise between available surface area to react the gases and surface area to which the particles could impact and adhere. Also, it is a channel diameter which has been used previously and is commercially available. The coal particle diameter was taken as 70 microns, the mean size of a standard pulverized coal supply. Smaller mean size coal particles might have less potential for impact and deposition in the bed. However, finer coal particles require more grinding energy which is not desirable from an energy usage point of view. Hence, the initial calculations were made with standard mean size coal particles. Later calculations utilized 25 micron diameter coal particles.

Examining Figure 2 it is noted that the solution curves for each air/fuel ratio are multivalued in temperature for a given bed length. This behavior is typical of chemical reactors where the upper temperature branch represents a stable solution and the lower branch represents an unstable solution which cannot be achieved during steady state operation. The third solution, which is also stable, is the unignited state, which occurs at a low temperature. This third solution is not of interest and does not appear on the figures. The stable and unstable solution curves meet at a bed length below which a hot stable solution cannot exist. Thus, for each air/fuel ratio a minimum bed length for stable operation can be defined. The minimum bed length results taken from Figure 2 and presented in Figure 3, show that, for a fixed coal feed rate, as air/fuel ratio is increased, the minimum bed length increases. This is primarily a result of increasing air mass throughput and thereby velocity in the bed as air/fuel ratio increases. The higher velocity shortens the residence time of the coal-air mixture for a given bed length, thereby reducing the

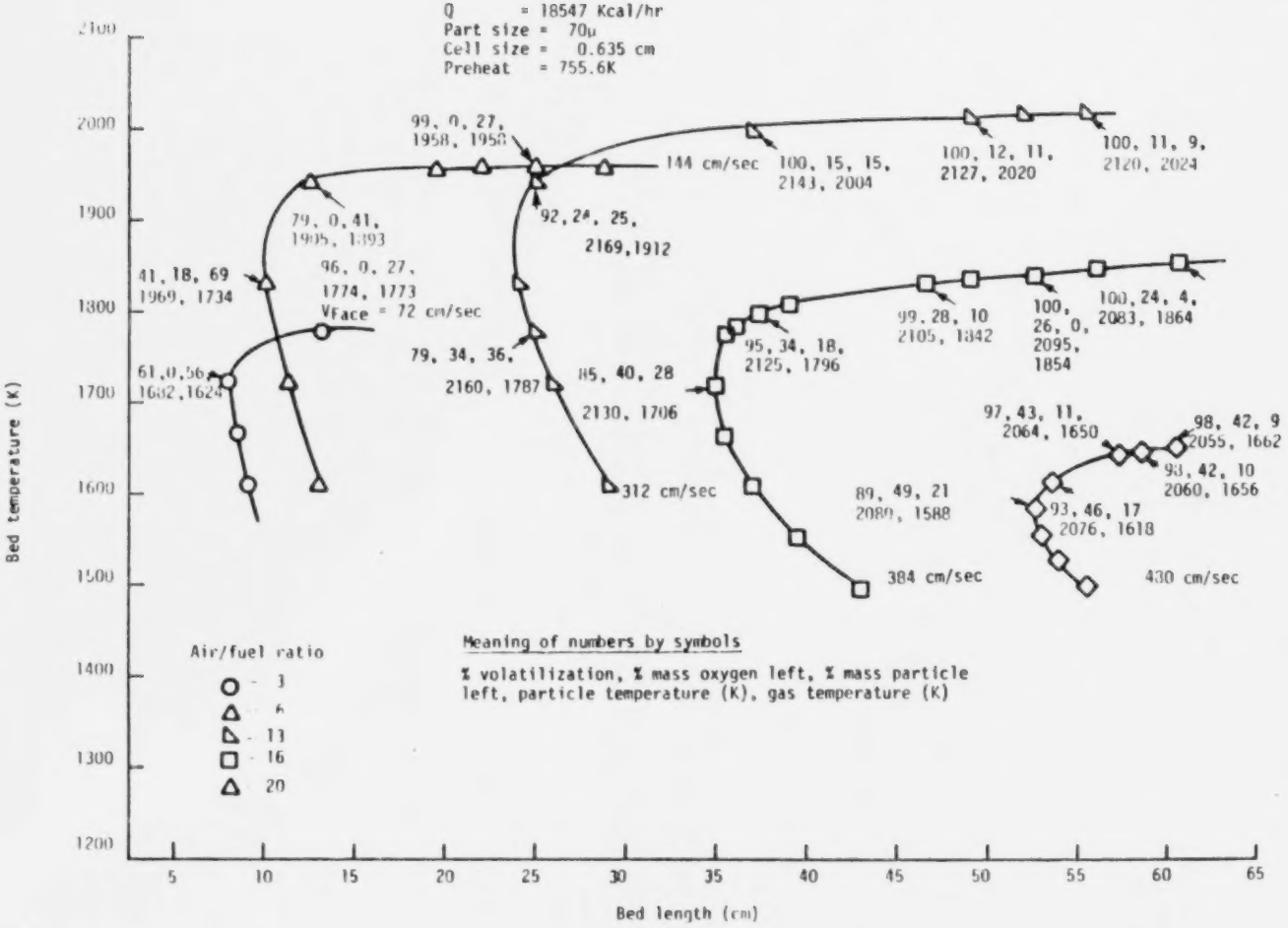


Figure 2. Constant coal flow combustor length map for 70 micron particles.

TABLE 1. COAL CHARACTERISTICS

| | Utah | | Western Kentucky |
|---|---|---|---|
| | Coarse | Fine | Standard |
| Particle diameter, μm | Weight % remaining on screen | | |
| 150 | 11.9 | 0.1 | -- |
| 75 | 46.5 | 3.1 | -- |
| 45 | 69.0 | 20.6 | -- |
| Mean | 90 | 30 | 70 |
| Composition weight % | | | |
| Carbon | 68.0 | 68.1 | 69.86 |
| Hydrogen | 5.2 | 5.2 | 4.86 |
| Oxygen | 14.7 | 14.4 | 8.73 |
| Sulfur | 0.64 | 0.63 | 2.98 |
| Nitrogen | 1.38 | 1.40 | 1.31 |
| Moisture | 2.64 | 2.89 | 5.10 |
| Ash | 7.64 | 7.70 | 7.15 |
| Volatile matter weight % | 41.6 | 41.4 | 37.83 |
| HHV (kJ/kg) (Btu/lb) | 29,187 (12,560) | 29,120 (12,531) | 28,699 (12,350) |
| Stoichiometric air requirement as received (kg/kg) | 9.08 | 9.10 | 9.54 |

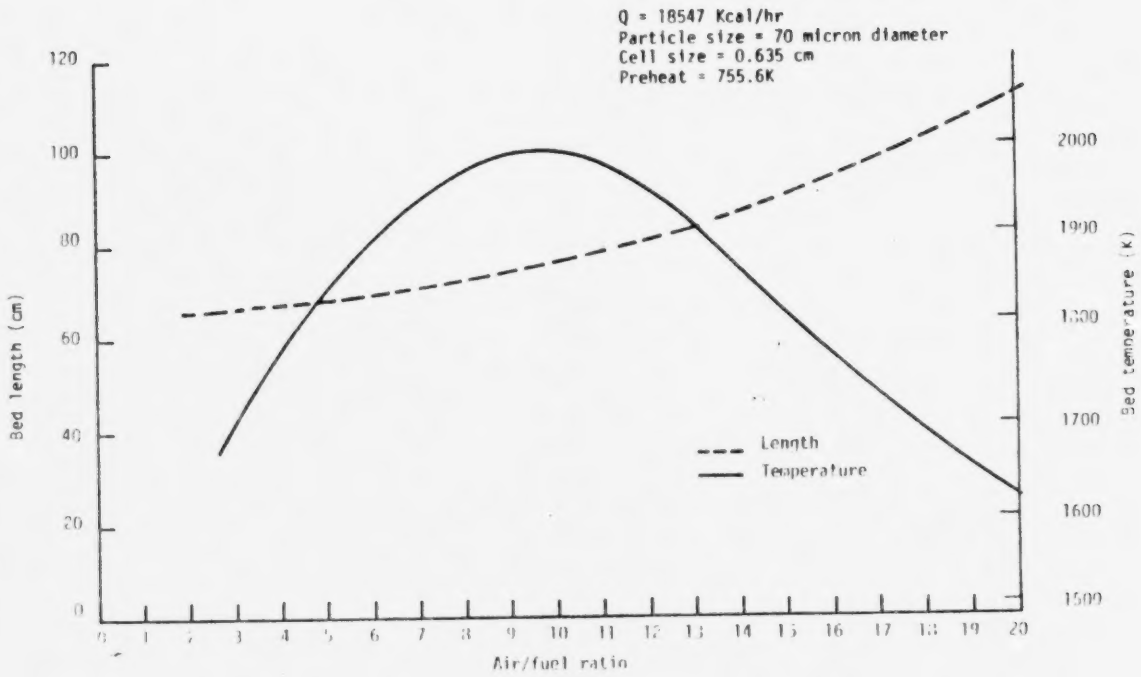


Figure 3. Minimum bed length and temperatures for stable operation for various air/fuel ratios.

degree of coal reaction. From these results it is obvious that for high bed face velocities, and the conditions as listed on Figure 2, long bed lengths are required.

Returning to Figures 2 and 3, it can be seen that stable bed operating temperatures range from approximately 1600K to over 2000K depending on air/fuel ratio. Since present material technology limits bed operating temperatures to roughly 1900K, these results show that bed overtemperatures could occur at air/fuel ratios somewhere between 6 and 13, depending on bed length. This is roughly indicated in Figure 3 by a plot of bed temperature at the minimum required bed length as a function of air/fuel ratio.

For bed lengths at which the combustor will operate stably, temperatures for most air/fuel ratios will not be much below maximum bed operating temperatures as limited by present material technology. Thus, the operating temperature regime for catalytic coal combustors is fairly narrow. Of course, these conclusions only apply to the nearly adiabatic* combustor case which was the condition of the calculations.

Also included on Figure 2 are some pertinent combustor exit condition predictions of percent coal volatilization**, mass fraction of initial oxygen and coal remaining and particle and gas exit temperatures. These results show that the minimum combustor length at a given air/fuel ratio only gives a partially combusted mixture, and greater lengths are required for more complete*** consumption of the coal. Also, particle exit temperatures, especially near the minimum length, are higher than gas exit temperatures. This is characteristic of heterogeneously ignited coal particle temperatures which overshoot gas and wall temperatures in the bed.

A typical distribution of gas and particle temperatures along the bed is given in Figure 4 along with percent volatilization and oxygen and particle mass consumption. These curves show that particles in the prebed section are heated by radiation from the front of the bed and the particles in turn heat the gas. The temperature rise of the particles and gas in the prebed section is fairly small, being of the order of 100K. However, once the particle/gas mixture enters the bed it is rapidly heated to high temperature by convective and radiative heat transfer from the hot walls. For the operating conditions as listed on Figure 4, significant volatilization occurs 6 cm into the bed. At 8 cm into the bed particle temperature is sufficient to cause significant heterogeneous combustion of the particles which further increases particle temperature above the bed temperature. The hot particles then heat the gas which in turn transfers heat to the bed. At the bed exit, both particle and gas temperatures are

---

*In the model, heat loss is only allowed through radiation from the front end of the bed to the upstream cold duct.

**Complete volatilization represents 70 percent of initial coal mass in these calculations.

***Complete with respect to available oxygen.

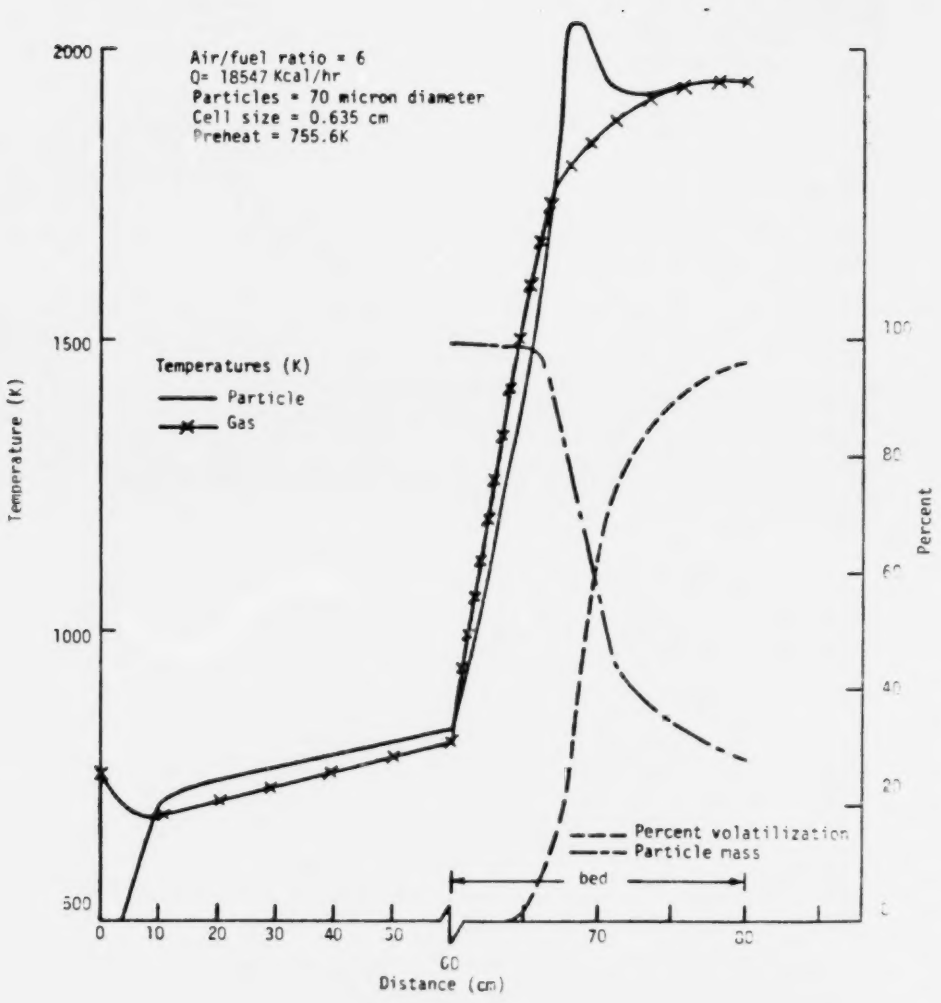


Figure 4. Temperature, volatilization and particle mass histories along bed.

near the bed temperature and volatilization is nearly complete with significant consumption of the coal having taken place.

Recognizing that impractically* long combustors would be needed to combust the coal at the high A/F ratio and velocity conditions as presented in Figures 2 through 4, constant low face velocity calculations were carried out over a range of air/fuel ratios. Conditions were the same as previous calculations except the face velocity was held constant at 72 cm/sec. The results of these calculations are presented in Figure 5. Reasonable combustor lengths are predicted for this low velocity case. This is expected since the residence time in the bed for these cases will be greater than that found in Figure 2 and will be of approximately the same level** for all the cases. The bed temperatures for the constant face velocity cases are below those found at high velocities. This is the result of the lower velocity cases having a higher proportionate heat loss to the upstream cold duct. Of course, a real combustor would lose heat in the radial direction as well as upstream. As previously mentioned, the radial heat loss is not accounted for in the model.

Combustor exit conditions for the constant face velocity minimum bed length predictions are presented in Figures 6 and 7 as a function of air/fuel ratio. Figure 6 shows that as air/fuel ratio increases, particle, gas, and bed exit temperatures first increase and then decrease with a maximum occuring between air/fuel ratios of 6 and 8. It should be noted that stoichiometric combustion with respect to the volatiles alone occurs at an air/fuel ratio of 6.3 and stoichiometric combustion with respect to the total coal occurs at an air/fuel ratio of 9. For these cases the maximum temperatures occur closer to the volatiles stoichiometric condition. In all cases, except at low air/fuel ratios, the particle temperature is greater than the gas temperature which is greater than the bed temperature. As mentioned previously, this is due to heterogeneous combustion which heats the particles above both the gas and bed temperature. At the combustor exit the heterogeneous process is still occurring and the bed, gas, and particle temperatures have not yet approached each other. Of course, wall reactions of volatiles are also contributing to overall combustion heat release in the model predictions.

Figure 7 gives the percent particle volatilization and percent consumption of oxygen and particle mass in the bed as a function of air/fuel ratio. Also included on this figure is a curve indicating particle mass loss due to volatilization alone. These results show that, at low air/fuel ratios, the coal consumption is due primarily to volatilization with little contribution from the heterogeneous oxidation reaction. As the air/fuel ratio increases beyond a ratio of 6, the heterogeneous oxidation of the coal contributes significantly to coal consumption. The more significant contribution of heterogeneous reactions at higher air/fuel ratios is also evident in Figure 6, where particle

---

* For the present experimental system
**Roughly 0.2 to 0.3 seconds for 20 cm bed length

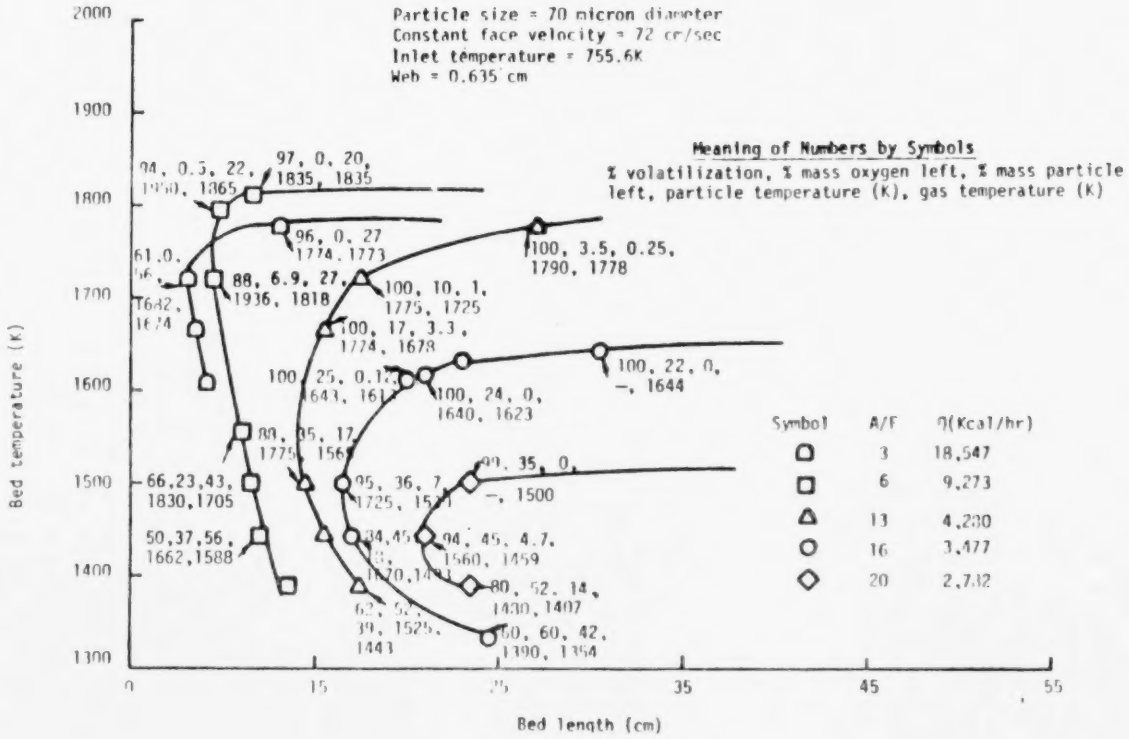


Figure 5. Constant airflow combustor length map for 70 micron particles.

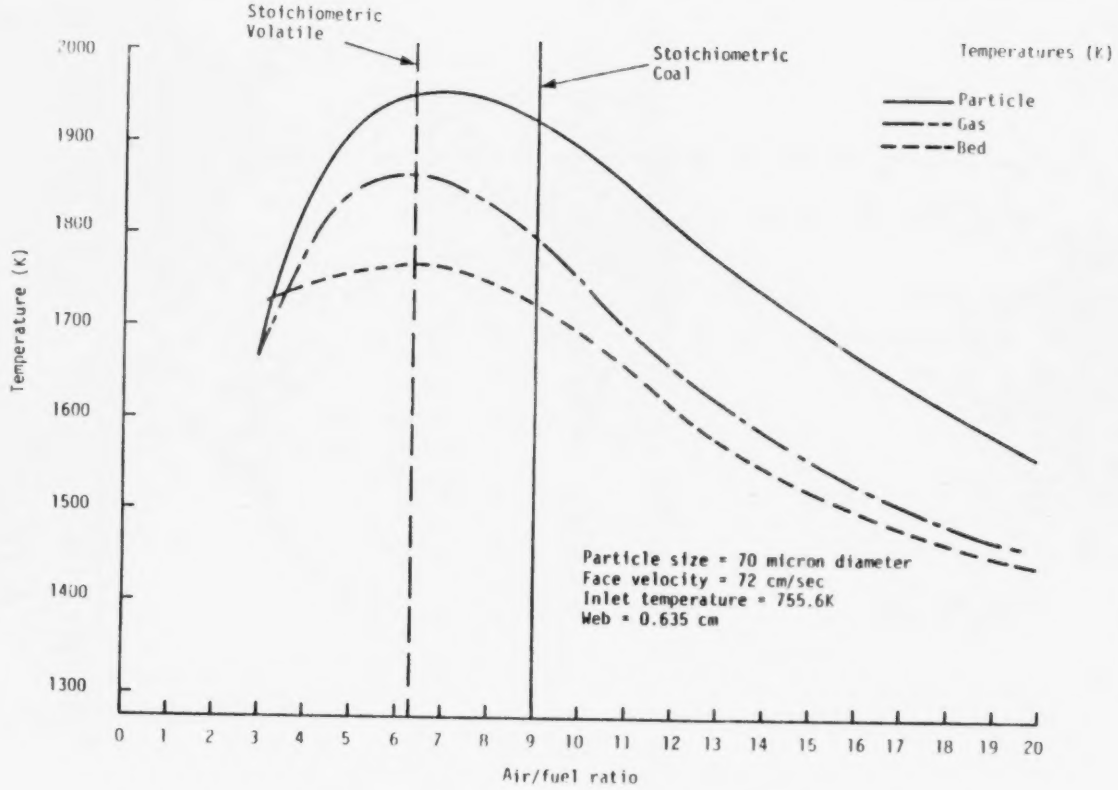


Figure 6. Minimum bed length particle, gas, and bed exit temperatures for various air/fuel ratios.

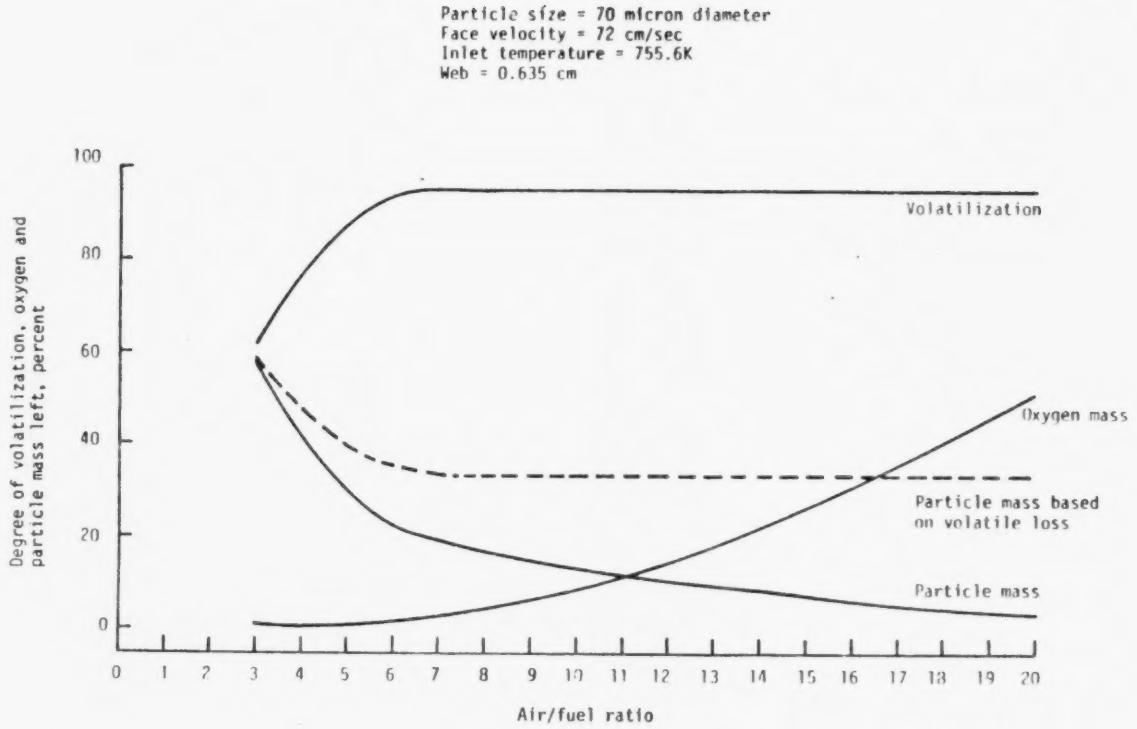
Particle size = 70 micron diameter
Face velocity = 72 cm/sec
Inlet temperature = 755.6K
Web = 0.635 cm
Degree of volatilization, oxygen and particle mass left, percent
100
80
60
40
20
0
Volatilization
Oxygen mass
Particle mass based on volatile loss
Particle mass
0 1 2 3 4 5 6 7 8 9 10 11 12 13 14 15 16 17 18 19 20
Air/fuel ratio

Figure 7. Minimum bed length percent volatilization, particle and oxygen mass left at combustor exit.

temperature at high air/fuel ratio is much higher than gas temperature. At low air/fuel ratios the primary heat release occurs by coal volatile combustion.

In addition to the 70 micron particle results, 25 micron coal particle predictions were also carried out to determine the effect of reduced particle size on combustor performance. Figure 8 presents the calculated bed temperatures achieved by different length combustors. These curves have a similar shape to those found for 70 micron particles presented in Figure 5. However, these curves have higher temperatures for a given length than the 70 micron results and the percent mass consumption of the particles indicates that the particles have been totally consumed.* The higher temperatures for the 25 micron particle cases are a result of less heat loss to the upstream duct due to particle cloud absorption and the complete consumption is due to more rapid particle heatup and consumption for the smaller particle size. Results for low air/fuel ratios are not presented since, in these reduced particle/gas mixture thermal mass cases, particle heatup was extremely rapid and the particles were fully reacted in the prebed section. Of course, this situation was not of interest in this study. At a velocity 3-times higher than the cases presented in Figure 8, the 25 micron particles were not fully reacted in the prebed chamber even at an air/fuel ratio of 3. Figure 9 shows that at this high velocity, a bed over 10 cm long is needed for stable combustion. It should be noted that, for this nearly adiabatic case, the bed temperatures for air/fuel ratios of 3 and 13 will be at or above the upper material temperature limit. Also, bed lengths required for stable operation with 25 micron particles are significantly shorter than those required for 70 micron particles.

## 2.4 CONCLUSIONS

In conclusion, for 70 micron diameter particles and 755K preheated air, bed lengths of 20 cm require prebed section velocities of 300 cm/sec or less for stable combustion at air/fuel ratios above stoichiometric. Of course, this conclusion is for a monosized coal supply. The predictions for 25 micron diameter particles show that velocities can be increased by a factor of 3 over the 70 particle size case and stable combustion will still be achieved for short bed lengths. These results indicate that a polysized coal supply, due to the presence of fine size particles, might have a wider stable operating range than a large particle monosized coal supply.

Another major conclusion of the analysis is that the operating temperature limits of the combustor are fairly narrow. High temperature is needed to activate the coal volatilization and heterogeneous oxidation reactions. However, the upper temperature is limited by catalytic bed

---

*The less than 100 percent volatilization figure at complete consumption indicates heterogeneous combustion was faster than volatilization for these cases.

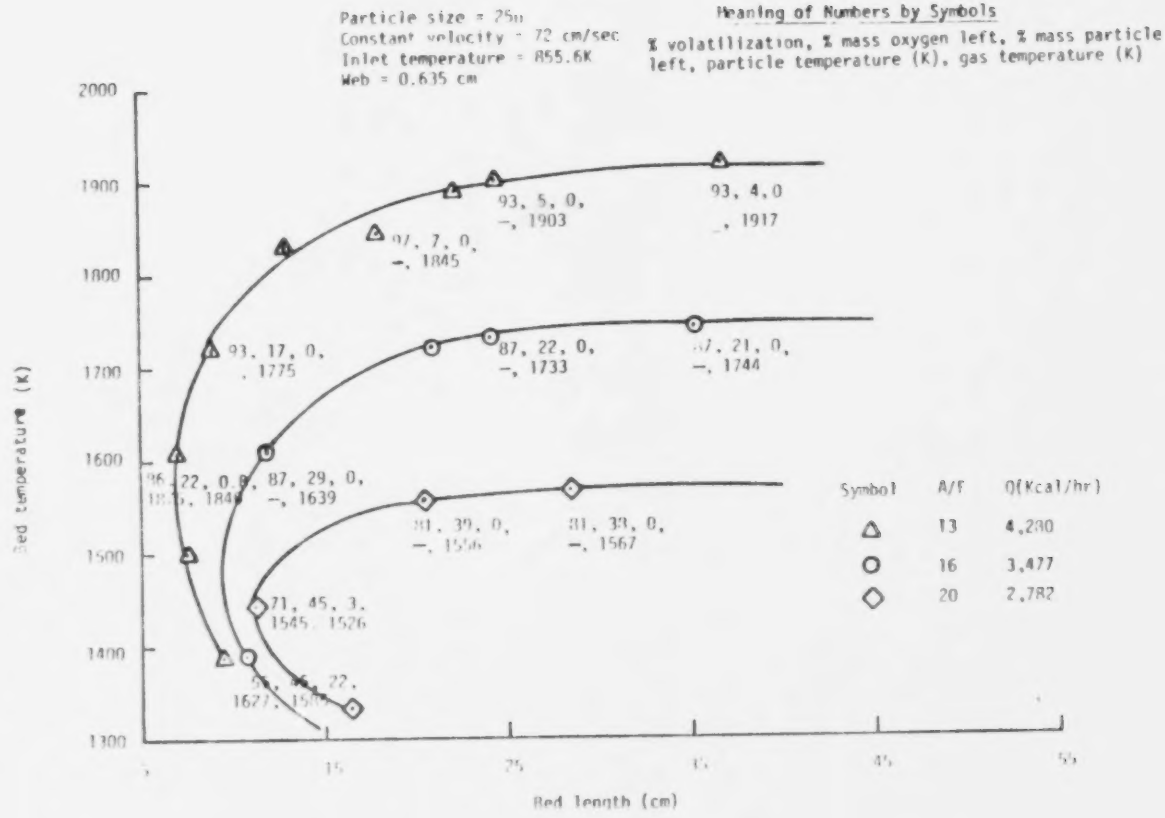


Figure 8. Constant airflow combustor length map for 25 micron particles.

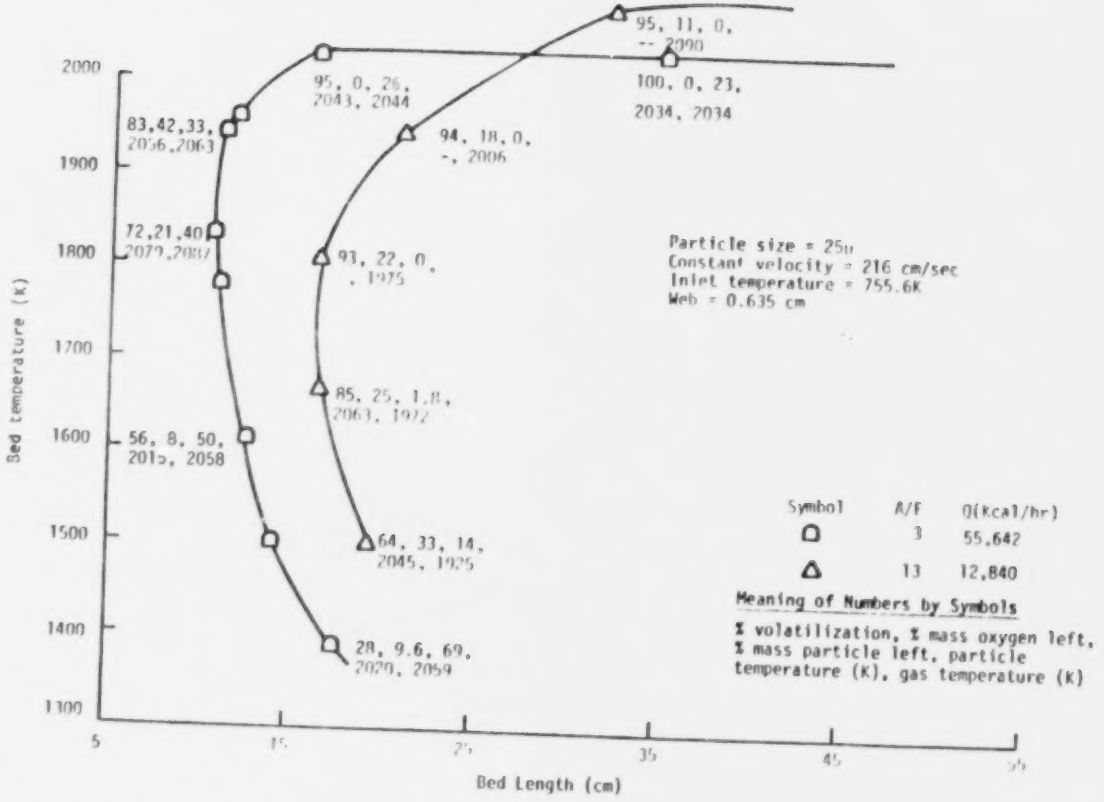


Figure 9. Constant high airflow combustor length map for 25 micron particles.

material temperature limits. For substoichiometric operation and 70 micron diameter coal particles the width of the operating temperature range is at most 300K. For 25 micron particles at higher velocities this operating range shrinks to less than 100K. Of course, this is for the model's nearly adiabatic bed case.

Finally, analogous to gaseous or liquid-fueled catalytic combustors, the calculations show that the bed serves as an initiator of reactions. Once the particle and gas temperatures are driven above a certain level, particle heterogeneous reactions in the model take over to further increase temperature and complete the combustion process.

# SECTION 3

# FEASIBILITY TESTING

Guided by the analysis described in Section 2, an experimental system was designed, fabricated, and operated to assess the feasibility of burning coal in a catalytic combustor. For the most part, conventional catalytic combustor technology was used in developing the experimental system. During the testing, propane and air were used to heat the bed prior to coal addition. Once coal was flowing, the propane was turned off with the coal supplying all of the combustion heat release. The following subsections describe the experimental system and the feasibility tests.

## 3.1 EXPERIMENTAL EQUIPMENT

A schematic of the experimental set-up is shown in Figure 10. Mixtures of air, propane and/or pulverized coal are brought into the catalyst housing through a stainless steel expansion chamber. The expansion chamber has a minor diameter of approximately 2.54 cm and expands to a diameter of 9.8 cm.

Air and propane flow rates are monitored by rotameters. Before entering the expansion chamber the air passes through a heater section which can preheat the air to a maximum of 811K (1000°F). After the air passes through the preheater, propane is injected into the air line and the mixture then enters the expansion chamber. The expansion chamber is surrounded by a guard heater which prevents heat loss from the expansion section, thereby maintaining the air/propane temperature at the selected level.

### 3.1.1 Catalyst Housing

The expansion section leads into the catalyst housing which is connected to a water-cooled exhaust section. The catalyst housing is shown in Figure 11. The catalyst housing has a length of about 47 cm. It is constructed of castable refractory. An insulating blanket separates the refractory from an outside steel shell. The refractory has an inner diameter of 8.9 cm and a thickness of 2.39 cm. The top of the refractory expands to an inner diameter of 9.65 cm to mate with the expansion section. The insulating blanket has a thickness of 1.27 cm.

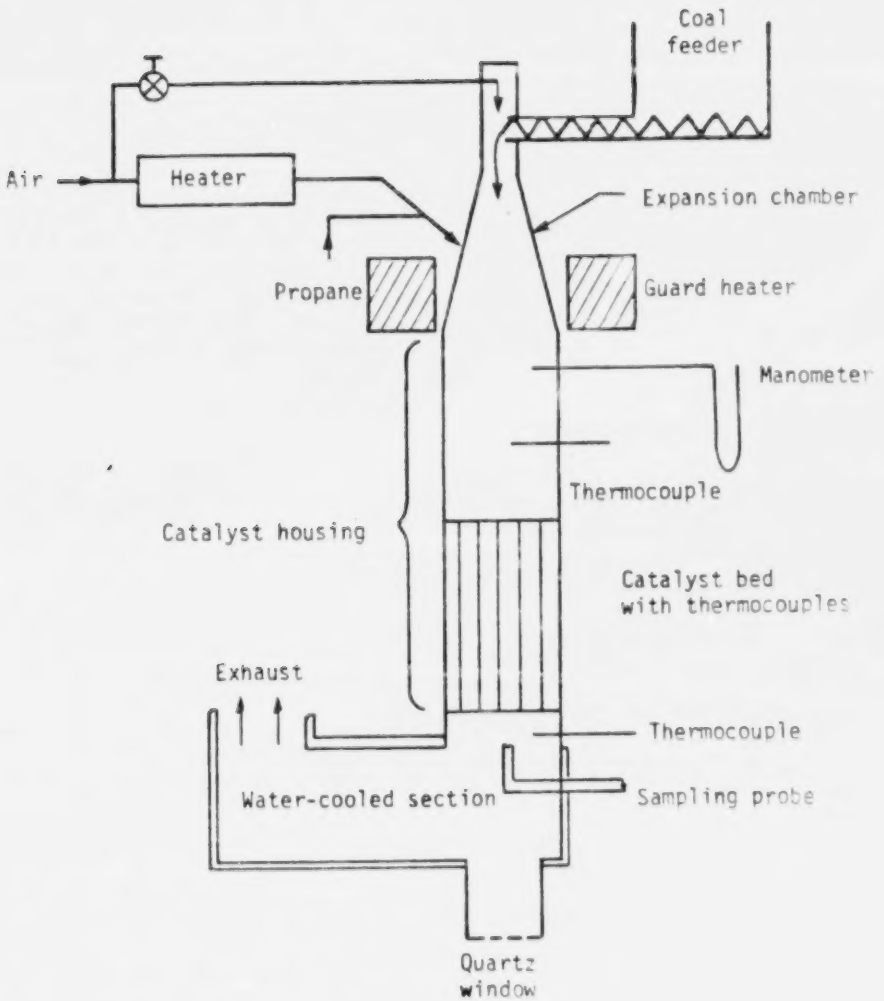


Figure 10. Combustion system flow diagram.

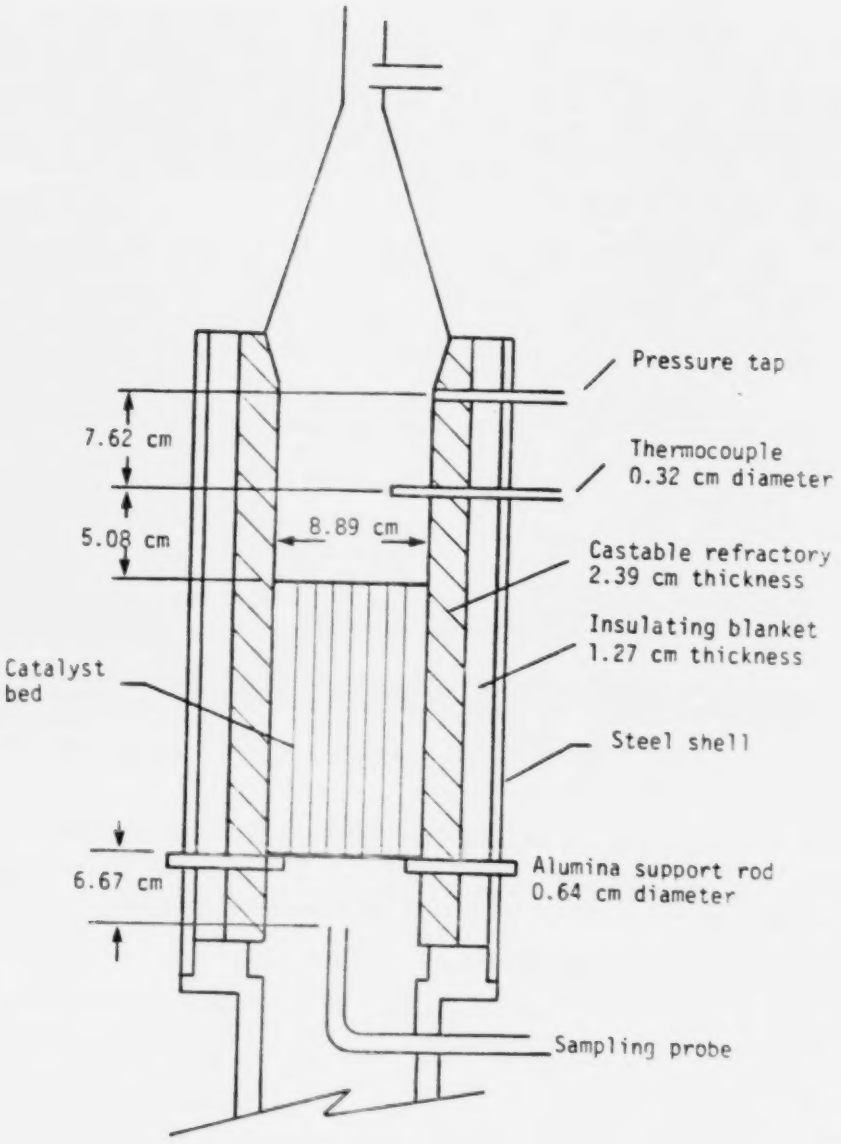


Figure 11. Catalyst housing.

### 3.1.2 Catalyst Beds

Two catalyst beds were used in the feasibility testing. Zirconia spinel monoliths, prepared by Corning Glass Works, were used as supports for the $Co_2O_3$ and platinum catalysts. Zirconia spinel has an upper temperature limit of 1978K (3100°F) and was felt to be an adequate material for this test program. The catalysts were applied to the monoliths without a washcoat. Both Pt and $Co_2O_3$ were used to give good activity over a broad range of temperatures maximizing the potential for successful operation.

The two beds had lengths of 21.6 cm and 17.8 cm, which, according to the analysis, would operate stably at reasonable preheats and flow rates. Each was fabricated using three sections of zirconia spinel monolith having 0.64 cm square cells and a void fraction of about 60 percent. The diameter of the monolith sections was 8.64 cm.

The monolith sections were joined end to end in a column using ceramic cement around the monolith periphery. When the sections were joined, care was taken to ensure that the internal 0.64 cm cells lined up without forming ridges between adjoining sections.

Several thermocouples (type K and R) were placed in the bed. They were located in one channel and positioned along the length of the bed. High temperature cement was used to hold the thermocouples in position. The front and back faces of the thermocouple channel were sealed with cement to prevent intrusion by any foreign materials.

The catalyst loading placed on the monoliths (before stacking) was fairly constant. The $Co_2O_3$ loading was typically 4.2 weight percent, while the platinum loading was 0.8 weight percent. The catalyst materials were applied in the forms of $Co(NO_3)_3$ and $H_2Pt\ Cl_6$, and calcined at 672K (750°F) before use.

Once the bed was instrumented with thermocouples and cemented into a column, the unit was inserted into the refractory tube, as shown in Figure 11. The bed was supported by 0.64 cm alumina tubes inserted into the four holes in the bottom of the combustor housing.

### 3.1.3 Sampling System

A schematic of the sampling system flow is shown in Figure 12. Gases and solids were withdrawn through a 0.95 cm diameter water-cooled stainless steel sampling probe. The leading edge of the probe was 6.6 cm below the bottom of the catalyst bed. Gases and solids were withdrawn at a rate of 0.3 $m^3$/hr. The sampled gases passed into a cyclone and fiberglass filter to remove particulates. The gases were then routed to $CO_2$, CO, $O_2$, NO and UHC analyzers. The analyzers and their capabilities are given in Table 2. The sampling lines, cyclone and filter were maintained at a temperature of 366K (200°F) to prevent condensation in the lines.

Samples were not withdrawn continuously. When not sampling, continuous air purging was used to prevent foreign materials from entering the probe.

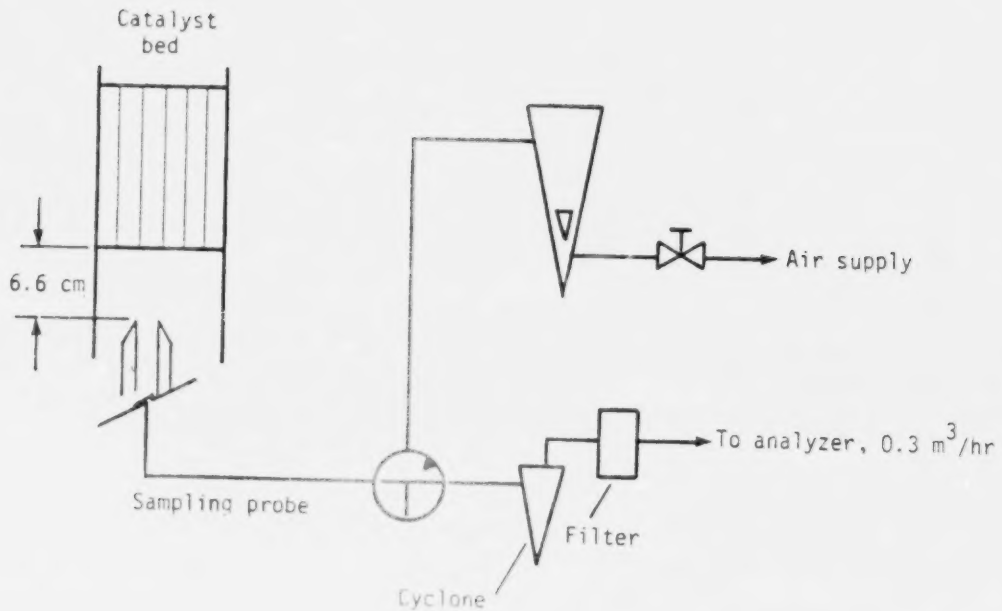


Figure 12. Sampling system flow.

TABLE 2. ANALYTICAL EQUIPMENT USED

| Chemical Species | Method | Detection Range | Equipment Model |
|---|---|---|---|
| CO | Infrared Absorption | 0-2000 ppm | Hartman & Braun Uras 2T/CO |
| $CO_2$ | Infrared Absorption | 0-20% | Hartman & Braun Uras 2T/$CO_2$ |
| $O_2$ | Paramagnetic Detection | 0-21% | Hartman & Braun Magnos 5T |
| UHC | Flame Ionization | 0-100,000 ppm | Beckman Model 400 HC Analyzer |
| NO, $NO_x$ | Chemiluminescent | 0-10,000 ppm | Air Monitoring Inc. Model 32 C |

On a few occasions, gases were withdrawn from the combustor at locations above the catalyst bed to monitor prebed burning. The probe head used in these instances was an uncooled 0.64 cm diameter stainless steel tube. The samples were withdrawn at 0.3 $m^3$/hr and passed through the cyclone and filter.

Samples were not always taken isokinetically since the sampling rate was fixed. Sampling rates ranged from isokinetic to twice the isokinetic rate over the range of experimental conditions. Since the objective of the particle sampling was to obtain composition and not mass loading, the deviation of sampling from isokinetic is not critical.

It should be noted that the extractive sampling probe head was designed to measure post flame gases of gaseous or liquid fuel fired catalytic combustors. Since coal takes a considerable time to burn completely, the gases and solids exiting the bed during this test program consisted of only a partially combusted gas/particle mixture. Sampling technology for partially burnt gas/particle mixtures is not yet fully developed. Water cooled probes, as in the current system, might not cool the mixture fast enough to freeze reactions and thus may not give a good in situ measurement. However, water quench probes, which inject water into the sampled mixture to achieve very high cooling rates might alter sample composition due to the presence of the water in the sample. Because of the limitations of both methods, it was decided to utilize the existing water cooled probe head. Some sampling error is bound to be present with this system. The limited knowledge of the accuracy of these types of probes when measuring partially burnt particle/gas mixtures does not permit a quantification of sampling error at this time.

### 3.1.4 Coal Feed System

Pulverized coal was fed into the combustor using an Acrison Model 105Z screw feeder. The end of the discharge tube of the screw feeder was located above the expansion chamber shown in Figure 10, and a small air jet was located above the end of the discharge tube. While feeding coal, the air jet is used to smooth out the fluctuations caused by the rotating screw. The concentration of the coal dust becomes even more uniform as it flows and disperses through the expansion section and into the combustor housing. Utah coal was the primary fuel used during this test program. Western Kentucky coal was used in some initial tests. Properties for these fuels are given in Table 1 which was presented in Section 2.

### 3.1.5 Temperature and Pressure Monitoring

Temperatures were monitored using thermocouples at several locations in the system. The temperature of the gases exiting the expansion chamber (preheat temperature) was monitored by a multi-sheathed type R thermocouple located in the gas stream at points either 6.9 cm or 14.5 cm above the front surface of the 21.6 cm bed or, 10.7 cm or 18.3 cm above the 17.8 cm bed. This thermocouple was also used to monitor any undesirable prebed combustion.

Static pressure was also measured at a location above the catalyst bed to monitor any bed plugging due to particle deposition. The probe was simply a 0.64 cm diameter stainless steel tube with one end connected to a manometer. The other end was inserted into the combustor housing so that the face was perpendicular to the flow direction. The tube protruded into the gas flow during the earlier tests but was later recessed into the refractory wall. Recessing the probe reduced any possibility of flameholding on the uncooled probe. The pressure tap height above the bed alternated between 6.9 cm and 8.3 cm depending on catalyst length and above bed thermocouple location. The static pressure probe was also used on several occasions as a gas sampling probe to get an indication of above bed gas composition.

The temperature of the mixture exiting the catalyst was measured by a type K thermocouple with an Inconel sheath. The tip of this thermocouple was located 6.4 cm below the bottom of the bed and 1.3 cm off the bed centerline.

## 3.2 FEASIBILITY TEST RESULTS

More than seventeen tests were conducted during the feasibility testing. Due to the exploratory nature of the experiments, test procedures were developed during the tests. Thus, each test series was conducted somewhat differently with some changes in thermocouple location and sampling position between tests. Because of these differences, specific test events are presented chronologically before the test results are discussed as a group.

### 3.2.1 Test Series 1

For this as well as the following test series a Western Kentucky coal of 70 mean diameter was used. A catalyst bed length of 21.6 cm was used, with the catalyst consisting of $Pt/Co_2O_3$ as described earlier. The bed was initially lit off catalytically with propane and air at an air preheat temperature of 594K (610°F) and an air flow rate of 54 $m^3$/hr. The air/fuel ratio was 40.

With the propane still flowing and the catalyst front end temperature at 1589K (2400°F) the coal flow was started. It was believed that a bed temperature of 1589K (2400°F) would be more than sufficient to initiate combustion. The coal flow rate was initially at 10 gm/min and was increased in step changes of about 12 gm/min every minute while carefully monitoring bed temperature until a coal flow of 55 gm/min was reached. The propane flow was reduced slowly with the airflow being reduced simultaneously in an attempt to maintain bed temperatures near the 1644K (2500°F) level. The air flow was reduced to 0.5 $m^3$/min and the propane flow to zero over a period of 20 minutes. This flowrate gave an air/fuel ratio of 0.98 and a face velocity of 6.64 m/sec.

During operation on coal, the bottom of the catalyst glowed uniformly indicating fairly uniform combustion and no plugging of channels. Also, at these conditions, chamber pressure was at a relatively low level of 1.5 cm water column, confirming that all channels were clear.

After about 15 minutes of operation on coal, the guard heater thermocouple unexpectedly reached a high temperature of 1139K (1590°F) and the bottom of the expansion section began glowing red. It was felt that significant combustion upstream of the bed was occurring which would lead to eventual failure of the upstream bed duct. Therefore, the coal flow was stopped at this point and the system shut down. Bed and gas temperatures while operating are presented in Figure 13.

These temperatures indicate upstream combustion to be occurring, followed by further combustion in the bed. This is indicated by the elevated bed temperatures as compared to the upstream and downstream gas temperatures.

After cooling, the bed thermocouples were found to be inoperative. At this point the catalyst was removed for reinstrumentation and inspection. Upon inspection, the walls of the catalyst prebed housing were found to be a bit discolored but showed no substantial ash accumulation. The front of the catalyst bed was relatively clean. However, some ash was loosely bound to the back end of the bed. This ash was stuck on in the form of droplets. A photograph presented as Figure 14 shows the front and back end of the bed.

The lack of significant deposits in the bed was encouraging. However, the upstream burning experienced during this initial test was defined as a problem in that it could cause prebed duct failure, plugging of channels with ash formed in the prebed section and obscuring of the effect of the catalytic bed on coal combustion. Thus, operating procedures for subsequent tests were modified to reduce the potential for prebed burning. Procedures modified for subsequent tests included:

- Very quick change over from gas to coal to avoid prebed heatup due to gas combustion at the low air flow rates needed for coal combustion
- Maintenance of higher prebed air velocity until gas had been shut off and the prebed section had cooled to prevent flashbacks.

It was believed that both of these changes would reduce the potential for prebed burning.

### 3.2.2 Test Series 2

Prior to this test series three additional thermocouples were installed while the bed was assembled so that positive contact between the bed and thermocouple bead was not assured.

Difficulty was experienced when trying to relight the catalyst bed after the test series 1 run on coal and air. Thermocouples indicated the top of the bed was relatively hot (922K (1200°F)) while the rest of the bed was cool (616K(650°F)). Observations through the viewport at the bottom of the combustor (Figure 10) showed only the front end of the bed glowing. A small bluish propane flame was visible at the back end of the

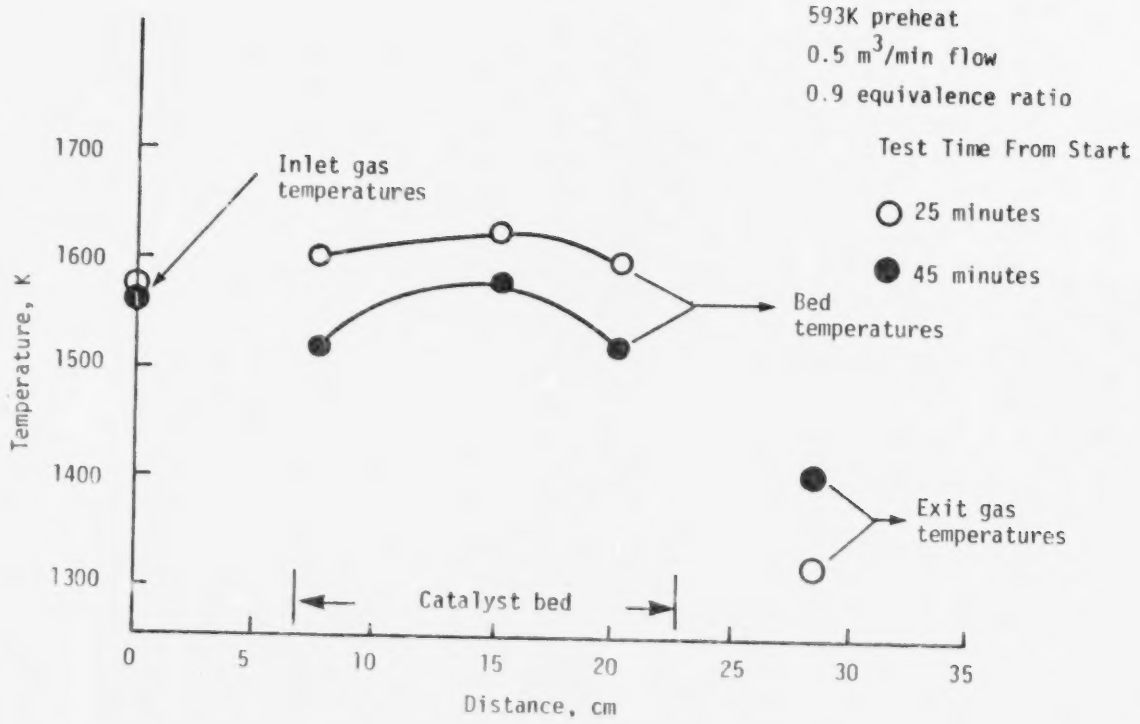


Figure 13. Bed and gas temperatures -- test series 1.

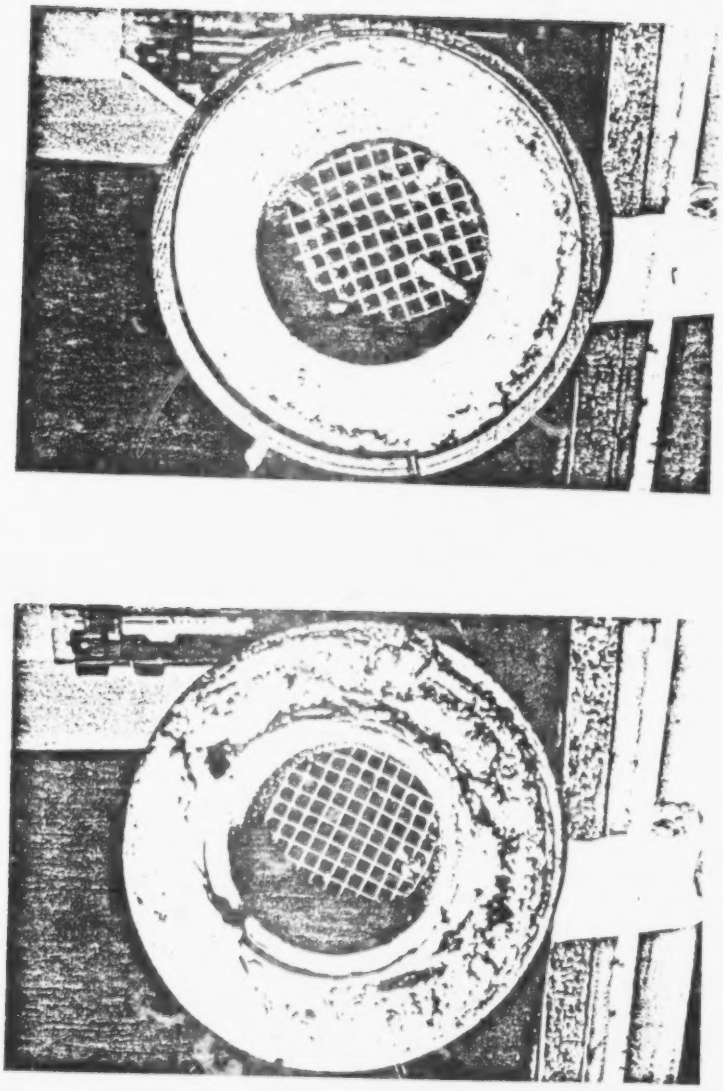

Figure 14. Post-test view of Test Series 1 catalyst bed.

bed which had a flat flame appearance. After a period of time, the bed front end temperature climbed to 1033K(1400°F) while the rest of the bed remained cool. The exhaust gas thermocouple indicated a temperature of 1422K(2100°F) which was probably the temperature of the attached propane flame downstream of the bed.

The low temperature measured near the back end of the bed during this test indicates a loss of bed catalytic activity. Either physical deposition of particulate, catalyst sintering or volatilization of platinum catalyst could have caused the loss of activity. The loss of $Co_2O_3$ catalyst would not be evident at the low bed temperatures measured since this catalyst is only active at high temperatures. However, the loss of platinum would cause a significant decrease in activity at low temperatures. Thus, the poor activity at low temperatures indicates that, at the very least, platinum has either been lost or deactivated on the back sections of the bed.

In an attempt to learn if coal combustion could be initiated at low bed temperatures, the coal flow was turned on and gradually increased. However, the coal flow was stopped quickly as temperatures in the bed dropped and bed pressure drop rose to about 8.9 cm w.c. (normally 1.3 cm w.c.) indicating significant particle deposition and plugging of the bed. It was obvious from this test that coal combustion initiation requires higher initial bed temperatures than those measured during this test.

In an attempt to burn out any coal blocking the bed channels, propane and air were run through the system for about two hours. During that time the pressure in the combustor began fluctuating but decreased slowly as the carbon burned away. Unfortunately, during this bed cleaning operation, all of the bed thermocouples became inoperative. At this point the pressure had decreased to 1.5 cm w.c. and the system was shut down.

After the system cooled, the quartz observation window (see Figure 10) was removed. Small rods of what appeared to be unburned coal were found among the char particles. Apparently, they were formed in the bed and had fallen out, possibly being the source of pressure fluctuations observed.

This test series showed that high bed temperatures are needed to initiate coal combustion in the catalytic bed. Also, unburned coal can deposit in and clog bed channels. However, most of the blockage can be removed by operating the bed at high temperature on propane with excess air. The coal burns away at these conditions, leaving behind an ash residue much smaller than the original coal plug. However, several plugging and cleaning operations might leave behind enough ash deposit to plug some channels.

### 3.2.3 Test Series 3

Before the next attempt to burn coal, the following modifications were made to the system:

- Five thermocouples were inserted in the catalyst bed to increase the probability of success for temperature measurements.

- In order to check for pre-bed combustion, provisions were made to withdraw gas samples through the tube previously used only to measure pressure. This tube was shortened so that it protruded into the combustion chamber about 2.5 cm.

- The Western Kentucky coal used in the first tests was replaced by Utah coal. The Utah coal characteristics are given in Table 1. Utah coal has been characterized in a number of EPA programs. It was used as the primary fuel in this program in order to permit easy comparison of the results of this program with the other programs using the same fuel.

- The bed was brushed with a platinum catalyst compound to increase the catalyst surface loading. This would increase the potential for successful gas lightoff and operation on coal during this test series.

The bed was lit off on propane with the main air preheat set at 601K (622°F) and the air flow at 33.6 $m^3$/hr and an A/F of 20. The temperature at the middle of the bed rose rapidly to 1566K (2360°F) with the pressure drop being 1.5 cm w.c. Observations showed the top of the bed was bright while the bottom was dull red. After about 20 minutes, the bed temperature at the front and back increased to 1650K (2510°F) and 1366K (2000°F) respectively. At this point the coal testing was initiated.

During this test series, seven tests were conducted with coal/air mixtures. Air/fuel ratios tested ranged from 4 to 10 and pre-bed velocities from 3.0 to 7.3 m/s. Preheat temperatures were kept between 616K (650°F) and 644K (700°F) for these tests. In seven of these tests, solid samples were collected along with gas samples.

Throughout this test series only quasi-steady conditions were achieved. Each of the tests was typically run for periods of 5 to 15 minutes over which time bed temperatures would continue to decline, indicating bed degradation. In general, the temperature of the bed could be increased by decreasing A/F ratio from an initially high value, or, to a lesser extent by increasing preheat temperature. However, increasing preheat caused burning above the bed. Decreases in A/F ratio served to raise the bed temperature, although once a particular temperature was reached, temperature decay began.

On some of the earlier runs in this test series, coal flow was stopped and propane flow started in an attempt to either heat the bed or maintain stable temperatures until the sampling cyclone was emptied and reconnected. Attempts to raise the bed temperature by propane addition were, for the most part, unsuccessful. If propane was introduced in quantities sufficient to increase the bed temperature, prebed flashbacks occurred. The propane operating conditions initially used to heat the bed could not be obtained after coal had been used. Reasons for increased flashbacks might be:

- Localized ignition sources created by coal firing which might include the prebed thermocouple, pressure probe, and coal ash deposited on chamber walls

- Increased upstream wall temperatures due to coal firing

Although the prebed thermocouple indicated high temperatures (up to 1005K (1350°F) in one case), gas sampling using the modified pressure tap indicated no combustion. However, the tap was located 7.6 cm above the thermocouple and therefore might have been outside the flame zone which the thermocouple measured. Also, the thermocouple might have been a site of localized flame holding, which would not be evident at the sampling port entrance upstream of the thermocouple.

Pressures ranged from about 1.8 cm w.c. (33.6 $m^3$/hr flow) at the start of the tests and 10 cm w.c. at the end (50.4 $m^3$/hr flow) indicating bed clogging due to particle deposition in the bed.

Inspection after the tests showed considerable ash deposits inside the bed. Figure 15 gives top and bottom views of the bed after the tests. The ash layers on the top and bottom of the bed were powdery while the ash inside the bed was much harder. The ash was arranged such that there was a greater deposit in the upper part of the bed than in the lower part. Ash was preferentially deposited around the perimeter of the catalyst, leaving the center sections fairly clean. It is hypothesized that coal is substantially combusted in the slow moving zones adjacent to the walls upstream of the bed. The ash which is exposed then has a high potential for sticking to the outer circumferential areas of the bed where velocities are low. This deposition builds up until the outer channels become clogged. Recirculation zones then form ahead of these clogged channels, increasing the amount of sticky ash formed upstream of the bed, as well as the potential for further clogging.

In addition, coal particles which are scattered off the front ends of the bed webs into the slow moving zones adjacent to the walls must also contribute to fouling. The void fraction of the bed is roughly 60 percent which gives a considerable solid frontal surface area off of which particle scattering, particularly large particle scattering, can take place. These particles should be scattered in all directions with a fraction of the larger particles reaching the walls where they can ignite and combust. These scattered particles can then contribute to the deposition and clogging problem.

It should also be noted that there was a relatively greater deposition at the top of the bed on the side opposite the entrance of the screw feeder, thermocouple and pressure tap. Obviously, coal feed distribution was not completely uniform in this system.

Friable ash deposits were also found on the lower sections of the exhaust thermocouple and the sampling probe. The combustor walls were relatively free of ash. However, some slight discolorations were noticed on the walls extending up past the prebed thermocouple, possibly indicating the extent of the recirculation zones.

The data collected during these tests are presented as a group in Section 3.3, including the data collected in test series 1, 2, and 4. Test series 3 strongly indicated that degradation of the catalyst and bed deposition and plugging were the primary problems which needed to be overcome for successful firing on coal. For the next test series it was decided to hold test conditions fixed over a long period of time. By monitoring bed temperatures and upstream and exit gas conditions over a period

Reproduced from
best available copy.

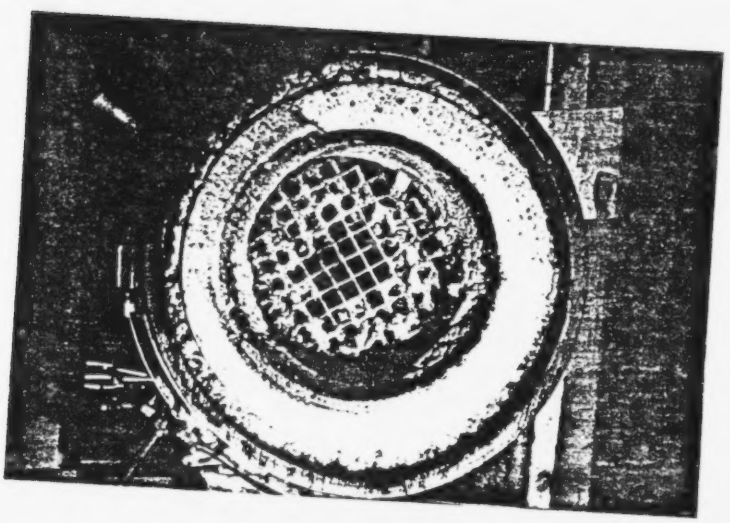

Figure 15. Post-test view of Test Series 3 catalyst bed.

of time, a clear picture of prebed combustion, catalyst degradation and bed deposition and plugging could be obtained.

### 3.2.4 Test Series 4

A new catalyst bed was placed in the combustion chamber. This zirconia spinel bed was similar to the old one, having a catalyst coating of Pt and $Co_2O_3$. The only difference between this bed and the previous bed was that the total length was 17.8 cm, or 3.8 cm shorter than the previous bed. This difference in length was not expected to change operating characteristics significantly. The bed was instrumented with 3 "R" type thermocouples and 3 "K" type thermocouples.

The upstream pressure probe/gas sampling probe position was changed for these tests. The pressure probe was located about 3.2 cm above the top of the bed. This change was made to ensure that prebed combustion in recirculation zones immediately above the bed could be monitored. The probe was mounted so that it protruded into a hole in the combustor wall. However, the leading edge was recessed in the hole by about 1.3 cm to avoid any chance of flame holding on the uncooled probe. The position of the sheathed thermocouple in the gas stream was located 10.8 cm above the bed, and 7.6 cm above the pressure probe.

The bed was lit on a propane/air mixture with the air flow at 50.4 $m^3$/hr and an A/F of about 40. The front of the catalyst bed was at a temperature of 1616K (2450°F) and the temperature difference between the back of the catalyst bed and the exhaust gas was about 360K with the exhaust temperature being lower.

During the first attempt in this test series to burn coal, the preheat temperature was raised to 731K (836°F) to learn if higher preheat would initiate coal combustion more rapidly and thereby speed the transition to coal only flow. When coal was started (air flow 33.6 $m^3$/hr, and 2.5 equivalence ratio) flashbacks into the duct occurred. The system was switched back to propane, the coal feed was turned off and the preheat was lowered.

The second try with coal was successful. The airflow rate was 57 $m^3$/hr and the equivalence ratio was 0.76. Preheat temperature was about 547K (525°F) and the bed face velocity was about 7.0 m/sec. The temperatures above and below the bed were 811K (1000°F) and 1088K (1500°F) respectively with the bed at a temperature of about 1422K (2100°F).

The bed in this test series was operated mostly on coal for a period of 6.5 hours. Bed face velocities were maintained between 5.5 m/s and 7.9 m/s with equivalence ratios spanning the range from 0.76 to 2.29. Preheat temperatures were held between 547K (524°F) and 691K (784°F) during these tests. Individual test conditions were held fixed for periods of up to 35 minutes to assess bed degradation during coal combustion as evidenced by bed temperature variations. This test procedure led to the following observations.

When operating on coal, the prebed gas temperature was observed to rise with time, indicating the presence of prebed burning. Upstream of the bed, gas sampling also confirmed that prebed combustion was taking place. Operating at high prebed temperatures over a period of time led to increases in bed pressure drop, indicating particle deposition and channel plugging were occurring. Eventually, the pressure drop rose to levels which required the termination of testing. Bed plugging was confirmed upon post test inspection of the bed. Figure 16 presents a post test photograph of the bed showing significant bed deposition and plugging.

As in previous tests, bed deposition and eventual plugging could not be avoided and testing had to be terminated. A further discussion of bed operating characteristics is given in the test results section which follows.

## 3.3 TEST RESULTS

During feasibility testing, two catalytic combustors were fired on coal for a total test time of approximately 6 hours each. The test conditions and data taken are summarized in Table 3. Equivalence ratios from 0.76 to 2.46 were run at total flowrates from 30 $m^3$/hr to 58 $m^3$/hr. These flows correspond to bed velocities of 3.0 to 7.7 m/s. Preheats, for the most part, were kept in the 603K (625°F) to 616K (650°F) range. Problems with preheat temperature control resulted in deviations from this level for several runs.

In nearly all cases the bed temperature was higher than the exit gas temperature, indicating heat release either on or near the catalyst surface. Bed temperature was measured at the periphery of the monolith and therefore bed temperatures represent minimum values. However, as mentioned previously, exit gas temperature measurement error may exist when firing on coal. The accuracy of the downstream gas temperature measurement has only been confirmed when firing on gas.

Degree of combustion based on sensible enthalpy change and ash tests of the solids collected indicate that, for most conditions, 20 percent or more of the fuel was combusted. It is expected that, for the short residence times in the bed, the major portion of the fuel combusted can probably be associated with the coal volatiles.

Several items should be noted concerning the data in Table 3. Test number 1 of test series 1 had very high prebed temperatures and therefore significant coal combustion probably occurred upstream of the bed. This condition is of little value in assessing the catalytic coal combustion process. However, it does provide a reference condition for the case where prebed burning is significant. Note that the highest extent of reaction, based on heat balance and ash tests, was achieved for this test case. Test number 1 of test series 4 is also unusual in that the high bed preheat led to moderately high prebed temperatures. As in the above case, prebed burning obscures the effect of the catalytic coal combustion process. Test 9 of test series 4 represents the last data point taken on a bed that had significant plugging and which had little heat release contribution from the catalytic bed. This data is included for completeness.

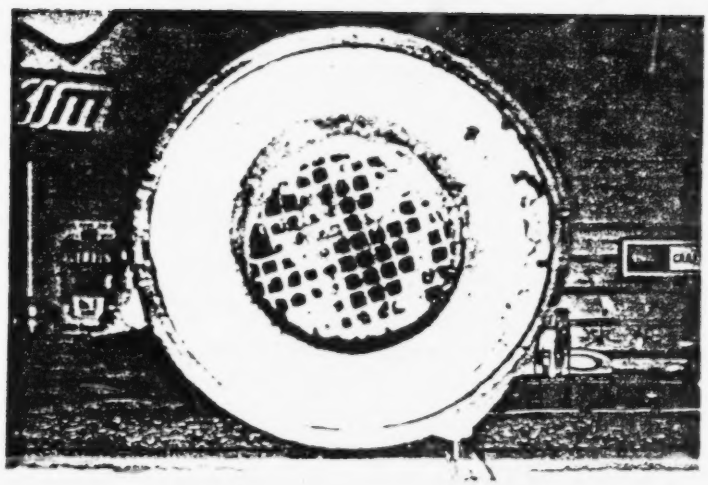

Figure 16. Top view of test series four catalyst bed.

TABLE 3. FEASIBILITY TEST DATA SUMMARY

| Test Series | Test No. | Equivalence Ratio | Air Flow Rate | Coal Flow Rate | Pre-bed Velocities | | Preheat Temp.[e] | Pre-Bed Temp.[e] | Bed Wall Temp.[e] | Exit Gas Temp. | Extent of Reaction | | | Exhaust Gas Composition | | |
|---|---|---|---|---|---|---|---|---|---|---|---|---|---|---|---|---|
| | # | $\Phi$[a] | $m^3/hr$ | g/min | $V_{1R}$[c] m/s | $V_1$[d] m/s | $T_1$ K | $T_{1R}$ K | $T_{3R}$ K | $T_7$ K | $N_q$[f] | $N_g$[g] | $N_{ash}$[h] | $O_2$ % | $CO_2$ % | NO, ppmv |
| 1 | 1 | 0.9 (10.6) | 30 | 56 | 6.64 | 2.53 | 594 | 1554 | 1587 | 1365 | 47 | 64 | 75.2 | 10 | 10.6 | 1160 |
| 3[b] | 1 | 0.98 (9.3) | 34 | 70 | 3.02 | 3.08 | 620<br>644 | 616 | 1337<br>1310 | 1375<br>1243 | 37 | 29 | 17.8 | 15 | 4.5 | 300 |
| | 2 | 1.19 (7.6) | 34 | 85 | 3.02 | 3.13 | 639 | 616 | 1476 | 1458 | 43 | 54 | 46.5<br>50.1 | 8.2 | 10 | 950 |
| | 3 | 1.44 (6.3) | 34 | 104 | 3.02 | 2.99 | 623<br>600 | 616 | 1462<br>1394 | 1457<br>139 | 42 | 24 | 40.4<br>41.3 | 14 | 6.5 | 1575 |
| | 4 | 0.88 (10.3) | 34 | 65 | 3.35 | 3.25 | 663 | 688 | 1387 | 1299 | 35 | 73 | 40.8 | 5.8 | 7.8 | 870 |
| | 5 | 0.78 (11.6) | 34 | 58 | 3.84 | 3.01 | 605<br>621 | 838<br>727 | 1337<br>1282 | 1258<br>1193 | 35 | 71 | | 8.0 | 10.9 | 391 |
| | 6 | 1.52 (6.0) | 51 | 165 | 7.16 | 4.57 | 616<br>622 | 977<br>949 | 1393<br>1321 | 1293<br>1232 | 32 | 36 | 36.7 | 8.0 | 10.9 | 587 |
| | 7 | 2.22 (4.1) | 51 | 240 | 7.32 | 4.48 | 602<br>619 | 1004<br>999 | 1296<br>1254 | 1193<br>1147 | 30 | 19 | 37.0<br>28.9 | 12.4 | 7.8 | 348 |

[a]Air/fuel ratio shown in parentheses
[b]Test series 2 attempt to run on coal was unsuccessful
[c]Based on prebed temperature
[d]Based on preheat temperature
[e]Plus and minus values indicate temperature range found during the test time at that condition. The first number represents the average value over the test time.
[f]Extent of reaction based on energy balance
[g]Extent of reaction based on gas composition
[h]Extent of reaction based on solid composition

TABLE 3. Concluded

| Test Series | Test No. | Equivalence Ratio | Air Flow Rate | Coal Flow Rate | Pre-bed Velocities | | Preheat Temp.[e] | Pre-Bed Temp.[e] | Bed Wall Temp.[e] | Exit Gas Temp. | Extent of Reaction | | | Exhaust Gas Composition | | |
|---|---|---|---|---|---|---|---|---|---|---|---|---|---|---|---|---|
| | # | $\phi$[a] | $m^3/hr$ | g/min | $V_{1R}$[c] m/s | $V_1$[d] m/s | $T_1$ K | $T_{1R}$ K | $T_{3R}$ K | $T_7$ K | $N_q$[f] | $N_g$[g] | $N_{ash}$[h] | $O_2$ % | $CO_2$ % | NO, ppmv |
| 4 | 1 | 2.46 (3.7) | 34 | 175 | 6.40 | 3.51 | 719 | 1310 | 1199 | 1249 | 29 | | | | | |
| | 2 | 0.76 (11.9) | 58 | 96 | 6.86 | 4.54 | 547 | 824 | 1429 | 1078 | 31 | 32 | | 15.4 | 2.0 | 109 |
| | 3 | 1.73 (5.2) | 44 | 160 | 5.43 | 3.84 | 603[d] ±9 | 852 ±58 | 1380 ±27 | 1041 ±49 | 24 | 14 | 23.2 | 15.4 | 2.4 | 1190 |
| | 4 | 1.73 (5.2) | 44 | 160 | 6.22 | 3.87 | 608 ±7 | 977 ±87 | 1374 ±12 | 1178 ±26 | 30 | 32 | 26.2 | 8.0 | 8.7 | 713 |
| | 5 | 2.29 (4.0) | 44 | 212 | 6.77 | 3.87 | 609 ±35 | 1067 ±35 | 1290 ±21 | 1065 ±62 | 25 | 21 | 29.4 | 9.7 | 4.4 | 374 |
| | 6 | 1.73 (5.2) | 44 | 160 | 5.67 | 4.27 | 671 ±24 | 890 ±35 | 1284 ±35 | 1265 ±23 | 30 | 15 | 57.9 | 15 | 3.6 | 250 |
| | 7 | 1.91 (4.8) | 51 | 204 | 7.74 | 5.06 | 690 ±5 | 1056 ±32 | 1390 ±34 | 1267 ±29 | 30 | 21 | 58.4 | 11.1 | 5.3 | 1125 |
| | 8 | 2.00 (4.5) | 34 | 142 | 5.61 | 3.20 | 653 | 1143 | 1268 ±43 | 1006 ±61 | 21 | 17 | 58.2 | 15.6 | 3.8 | 280 |
| | 9 | 2.00 (4.5) | 34 | 142 | 5.39 | 2.85 | 583 ±4 | 1064 ±11 | 1097 ±42 | 858 ±33 | 17 | 8 | 43.8 | 17 | 2.2 | 190 |

[a]Air/fuel ratio shown in parentheses
[b]Test series 2 attempt to run on coal was unsuccessful
[c]Based on prebed temperature
[d]Based on preheat temperature
[e]Plus and minus values indicate temperature range found during the test time at that condition. The first number represents the average value over the test time.
[f]Extent of reaction based on energy balance
[g]Extent of reaction based on gas composition
[h]Extent of reaction based on solid composition

### 3.3.1 Bed Temperature

During these tests, temperature and emissions data were taken every 5 minutes over the roughly 30 minute test period for each test condition to monitor any changes in bed operating characteristics. Figure 17 shows the variation of test series 4 temperatures with time as measured for fixed equivalence ratio and flow rate at three different times during the 6 hour test period. In between the test conditions presented in Figure 17, the bed was operated at other air/fuel ratios and briefly on gas while the sampling cyclone was cleaned. This is probably why temperatures do not match at the beginning and end of tests. It is apparent from these results that the prebed gas temperature, $T_{1R}$, rises with time indicating prebed combustion. However, even though prebed burning is occurring, the higher temperatures in the bed and exhaust duct indicate significant heat release in the bed. Also, since the bed temperature is higher than the exit gas temperature, catalytic wall reactions must be contributing to heat release.

Figure 18 shows the temperature histories of the test condition immediately following the last test in Figure 17 (test at 6:43 p.m.). At this new air/fuel ratio the bed operates similarly to that found for the previous test condition. Also presented on Figure 18 is the combustor pressure drop as a function of test time. The continuous rise in pressure drop for constant flow rate and moderate changes in temperature indicates that deposition of particles must be changing the geometry of the bed and plugging channels. When the pressure rose above 17 cm w.c. the coal flow was terminated and the system was switched over to gas.

Following a brief period, during which the combustor was operated on gas to clean the bed, coal flow was reinitiated and temperatures were monitored as before. These results, presented in Figure 19, show a very high prebed temperature, a lower bed temperature and a very low exit gas temperature when compared with the results in Figure 17. After shut down, visual inspection of the bed showed that significant channel plugging due to particle deposition had occurred. As indicated previously, it is hypothesized that in front of the plugged channels slow moving recirculation zones were established in which significant prebed combustion took place as evidenced by high local prebed temperatures. The ash exposed as a result of this prebed burning then had a high potential for depositing in the bed. This led to bed degradation and some channel plugging. The plugged channels then create higher velocities in the clear channels which then yield very low bed combustion efficiencies as evidenced by the reduced bed and exit gas temperatures.

In conclusion, the bed pressure drop results show that deposition can be significant within a one-hour period. Once deposition and clogging has been initiated, prebed burning becomes more significant, leading to further deposition and plugging. Eventually the bed is degraded to such an extent that it contributes little to the combustion heat release which then occurs primarily upstream of the bed in localized recirculation regions.

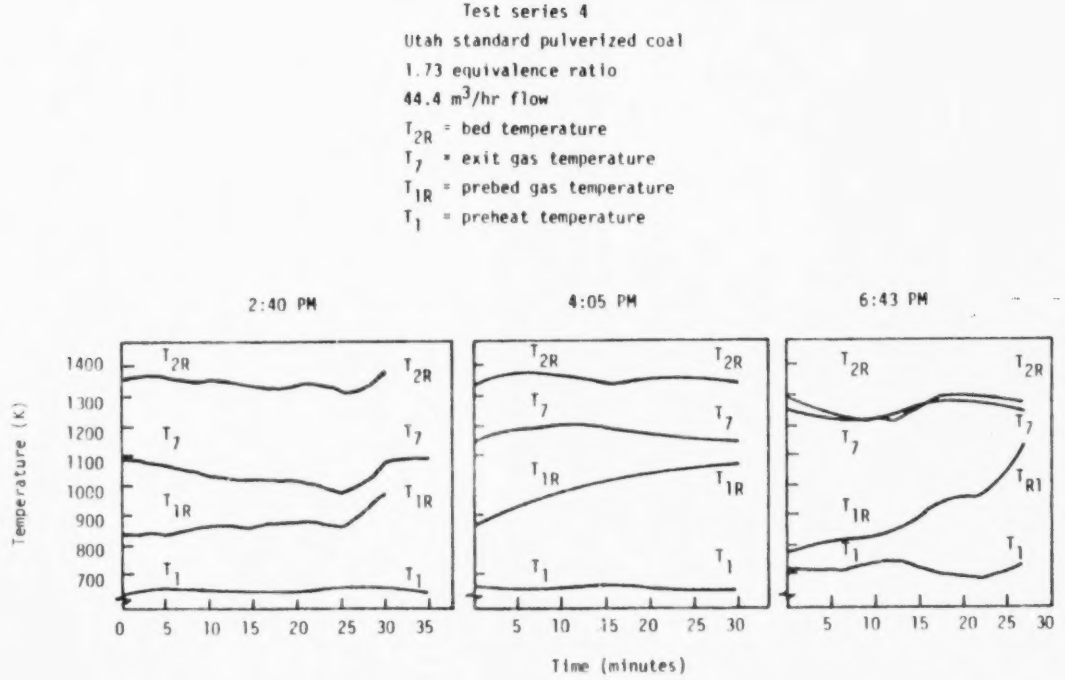


Figure 17. Variation of combustor temperatures with time.

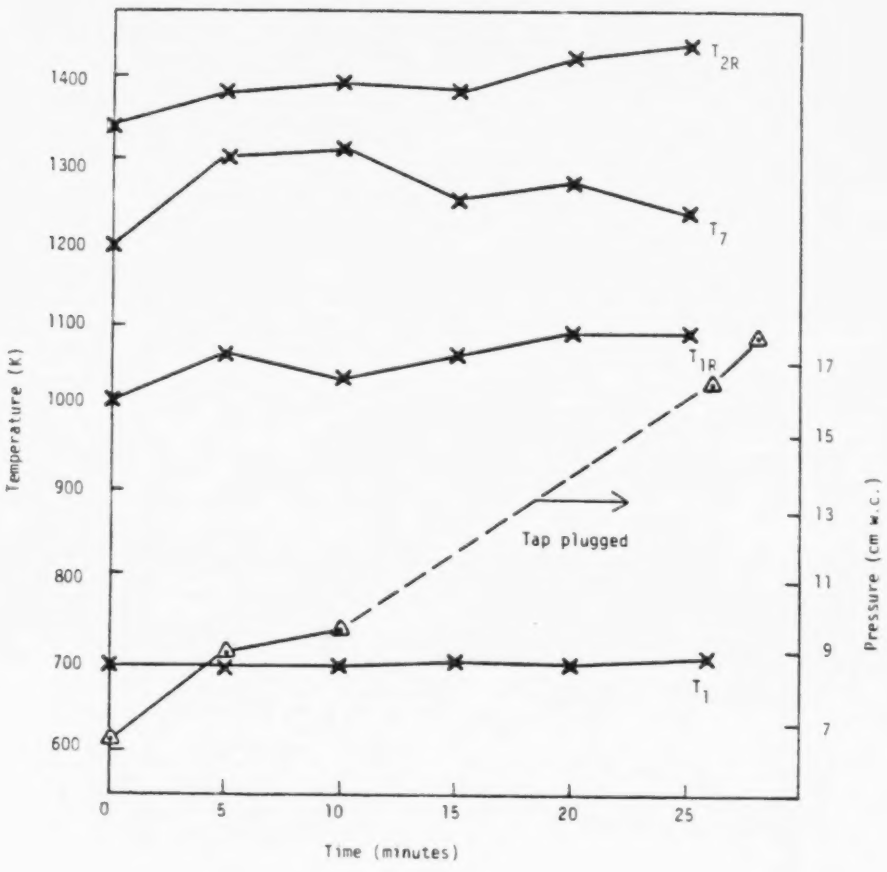


Test series 4
Utah standard pulverized coal
$\phi$ = 1.91
Q = 50.4 $m^3/hr$
$T_{2R}$ = bed temperature
$T_7$ = exit gas temperature
$T_{1R}$ = prebed gas temperature
$T_1$ = preheat temperature

Figure 18. Combustor temperature and pressure variations with time.

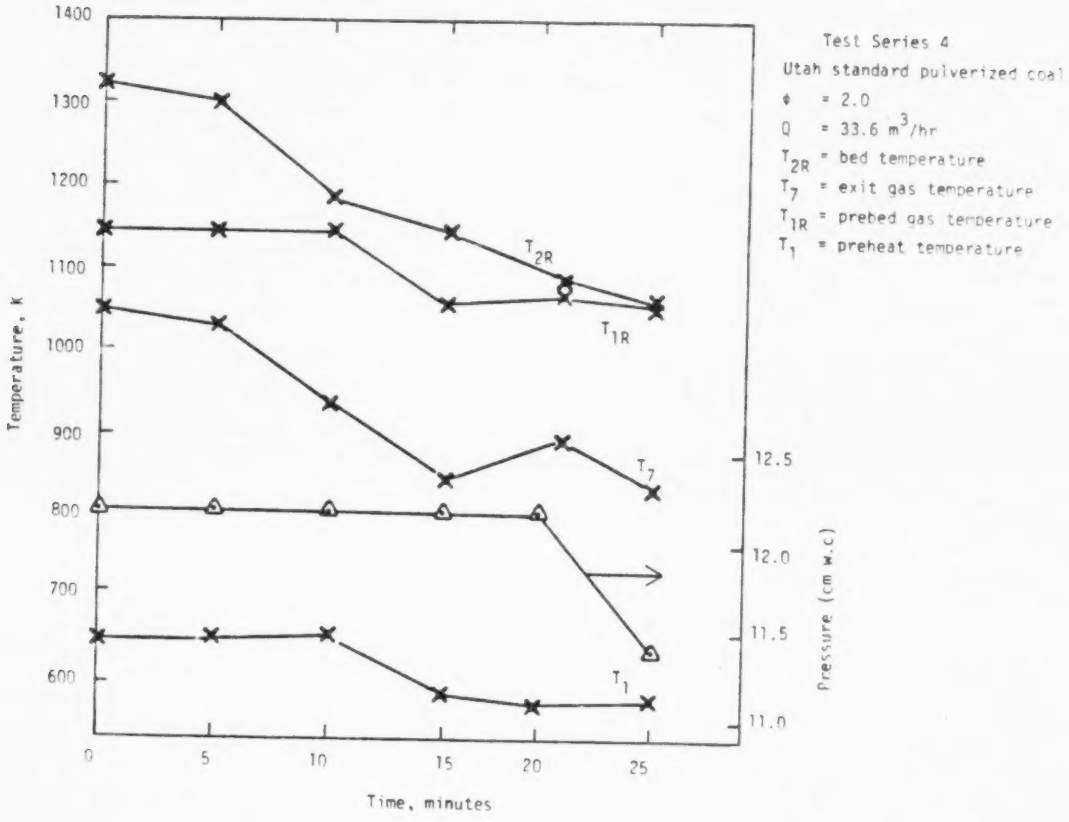


Figure 19. Variations of combustor temperatures with time.

### 3.3.2 Bed Pressure

During almost all of the tests using coal, the bed pressure was observed to rise gradually with time. However, a point would be reached where the rate of rise would increase, leading shortly thereafter to bed plugging. As discussed in the last section, this point occurs when particle deposition has created sufficient prebed low speed recirculation zones to cause significant prebed combustion. The ash exposed in these zones then has a high potential for deposition in the bed.

A plot of indicated pressure versus time for Test Series 4 is given in Figure 20. Over the course of the testing, which included both gas and coal firing, the pressure varied from about 1.3 cm to 22.9 cm w.c. This figure cannot be viewed as directly indicating the degree of bed fouling because of changes in flow rate and temperature with time. Figure 21 presents an estimate of the normalized channel clearance with time using the pressures indicated in Figure 20. Channel clearance was calculated assuming pressure drop was related only to velocity through the bed. It ignores changes in surface roughness, channel geometry, and solids loading. The temperature of the gas in the bed was assumed equal to the indicated exhaust gas temperature. The fraction of channels open is then given by:

$$\frac{N}{No} = \frac{f}{\Delta P} (QT)^2$$

where f is a constant, Q is the total volumetric flow of air, T is the temperature, and $\Delta P$ is the indicated pressure drop.

Figure 21 shows the fraction of open channels decreasing or blockage increasing with time. It also shows operation on gas tends to clear the bed. It was found in some cases that operation on gas for a few hours can almost completely unplug a bed. The last 30 minutes shown on Figure 21 corresponds to the last coal run (at time 7:45 PM) shown in Figure 19. Very significant plugging of this bed occured during this time period.

The ability to sometimes clear a plugged bed using gas provides information on the type of plugging process occurring. The initial plugging appears to be due to deposition of char. This char can be burnt out (or blown out by flashbacks) by operating the bed on gas under excess air conditions. However, burning out the char leaves behind small ash deposits in the bed. After clearing the bed of char several times the ash layer becomes substantial, which then alters the geometry and can lead to substantial prebed combustion. Once prebed burning is established, ash formed upstream can deposit in the bed. Of course, ash cannot be burnt off like char and once ash deposition becomes significant, the bed needs to be replaced.

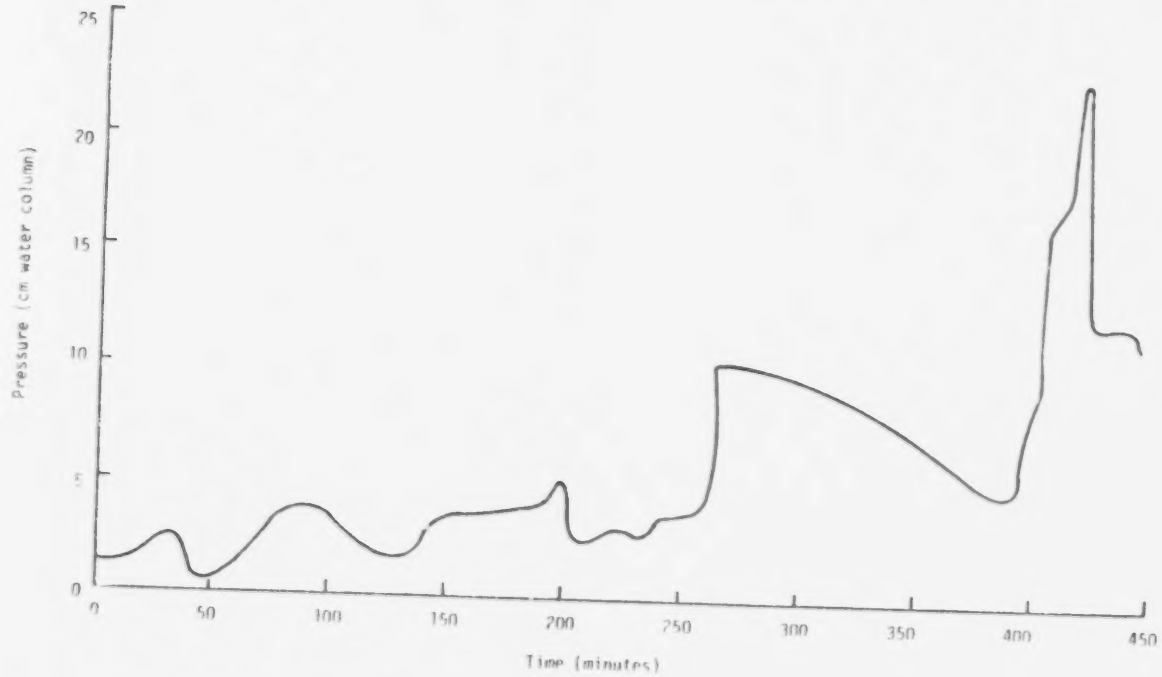


Figure 20. Prebed chamber pressure during test series 4.

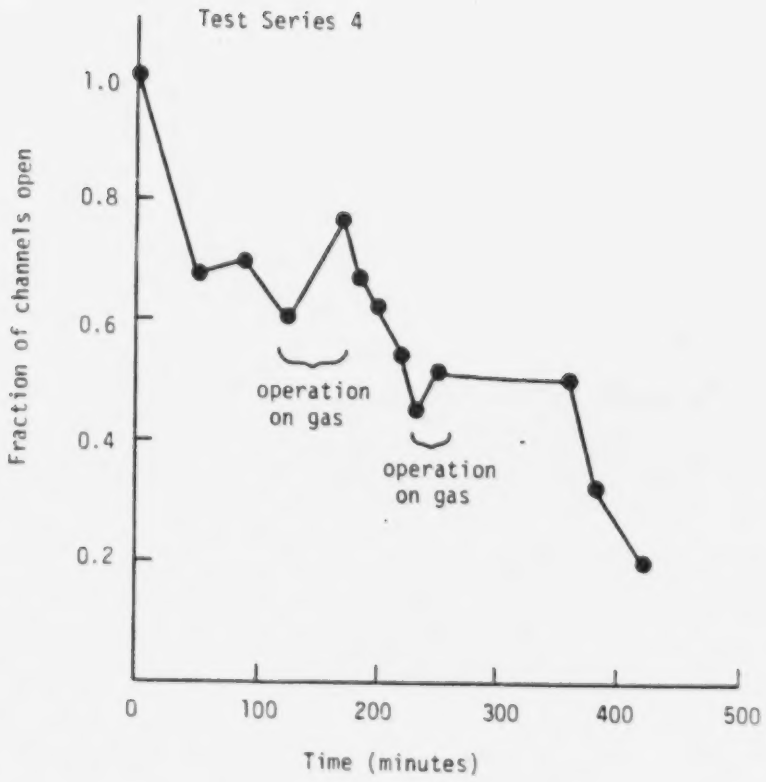


Figure 21. Fraction of channels open during test series 4.

### 3.3.3 Extent of Reaction

The extent of reaction of the coal during the feasibility testing was calculated by heat balance closure, ash tracer, and exhaust gas composition techniques. The results, as presented in Table 3, are seen to be somewhat inconsistent.

Extent of reactions based on a heat balance closure are subject to error due to heat transfer assumptions and approximations. For the results given in Table 3, convective and radiative heat losses from the test section outer steel shell and radiative heat losses from the bed front and back ends were included in the calculation. These losses are subject to temperature, heat transfer coefficient and radiative property uncertainties.

Combustion efficiencies using ash as a tracer should have less error than a heat balance. However, ash deposits dropping from the bed into the probe and ash volatilization can lead to errors. Also, ash tests give the percent weight loss of the coal which may not be equal to the extent of reaction if unburned fuel exits the combustor.

Exhaust gas results should yield reasonable extents of reaction. However, as noted previously, bed temperatures and hence operating conditions varied with time and the exhaust gas conditions represent a single isolated condition taken over the entire test time. Also, during these tests varying degrees of prebed burning occurred which cloud the effect of the bed on extent of reaction. Significant bed particle deposition and channel plugging events also occurred during testing and in test series 4 the bed length was changed which altered bed performance. The variability of bed operating characteristics with time, prebed combustion and the bed plugging problems made data collection and interpretation less than ideal during the feasibility testing.

Recognizing the inconsistencies of the extent of reaction results, Figure 22 presents these results for a range of air/fuel ratios. Included on Figure 22 are extents of reaction based on heat balance, ash tests and exhaust gas data. Also included on Figure 22 is a line indicating the theoretical maximum extent of reaction based on available oxygen. As expected, considerable scatter is evident in these results. Also, most of the data falls below the theoretical maximum line. However, three ash test results are higher than this line. This may be a result of some long time scale bed ash deposits falling from the bed into the probe, thereby enrichening the ash content of the particle catch sampled. Taken as a whole, it appears that the extent of reaction increases with air/fuel ratio up to an air/fuel ratio of 8. Above this air/fuel ratio, the extent of reaction, as determined by the bulk of the data, rises less rapidly and might even decrease as evidenced by some of the data. It is possible that, for the short bed residence times* of these tests, increased air/fuel ratios and hence increased thermal mass of the mixture slows down

---

*On the order of 30 msec residence time.

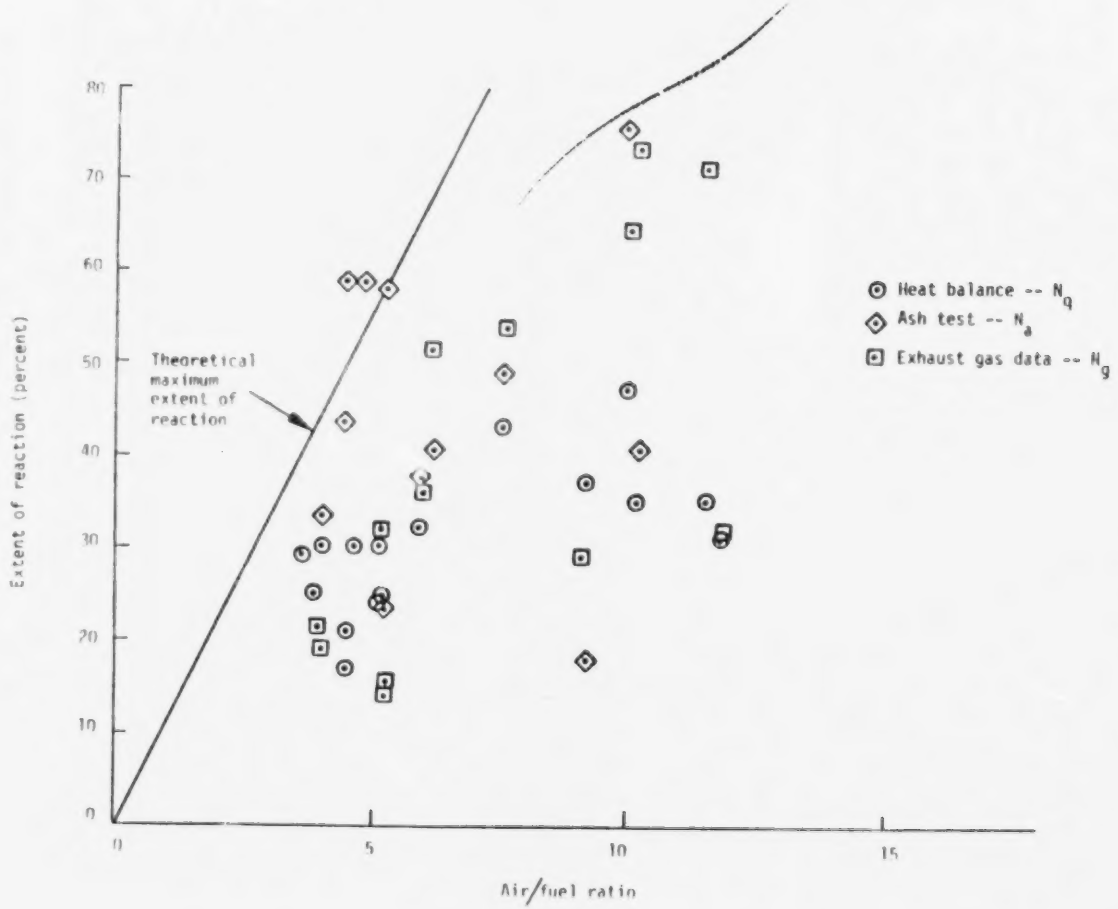


Figure 22. Extent of reaction versus air/fuel ratio for feasibility tests.

the temperature rise and thereby limits the extent of reaction. In conclusion, these results show that, for air/fuel ratios below 8, significant coal reaction takes place in this system.

As indicated previously, prebed combustion was present to varying degrees during most of these tests. Depending on where the combustion was initiated in the prebed section, the overall residence time under combustion conditions varied significantly during testing. This variation of residence time is probably responsible for some of the data scatter exhibited in Figure 22. Also, the prebed burning helps to maintain reaction even at high air/fuel ratios. As will be shown in the evaluation testing section, when prebed combustion was eliminated, the bed could not sustain combustion above an air/fuel ratio of approximately 6. The prebed burning during these tests increased the temperature of the mixture entering the bed and increased the residence time of the mixture at high temperature. Both of these processes are beneficial in terms of extent of reaction. However, as discussed previously, prebed burning leads to bed ash deposition and plugging which eventually seriously degrades the bed.

### 3.3.4 Emissions

As mentioned in the previous section, the gas data upon which extent of reaction is based exhibit significant scatter due to the nature of the feasibility tests. The NO emissions data also suffer from this same problem.

Figure 23 presents the NO emissions data for the full range of air/fuel ratios tested. These are uncorrected as measured NO levels. The data show that, in general, NO increases with air/fuel ratio under rich conditions, reaches a peak greater than 1000 ppm at an air/fuel ratio of around 6 to 10 and finally decreases to low levels at an air/fuel ratio of 12. The increase of NO with air/fuel ratio under rich conditions is consistent with conventional combustion results under rich conditions. This behavior might be due to the coal fuel bound nitrogen being reduced to $N_2$ or forming precursor species such as HCN and $NH_3$ rather than being oxidized to NO under fuel rich conditions. At the high air/fuel ratio combustion conditions the significant decrease in NO levels is not expected based on conventional combustion experience. However, conventional combustors have residence times on the order of seconds whereas the catalytic combustor has a residence time of about 30 milliseconds. Within this short residence time the coal can only partially react as shown in Figure 22 in the previous section. Thus, the low NO levels may be due to the fact that only a fraction of the coal fuel bound nitrogen has been released into the gas phase and has been converted to NO under lean conditions. This is somewhat substantiated by the results in Figure 24 which shows that NO is roughly proportional to extent of reaction. Of course, there is considerable scatter in the data and more lean condition data fall towards the low NO levels than the high NO levels. However, the general trend of the data shows that NO increases with extent of reaction.

In conclusion, the test results show that burning coal in a catalytic combustor produces NO levels which are high even under overall fuel rich conditions. This is probably due to the low system residence

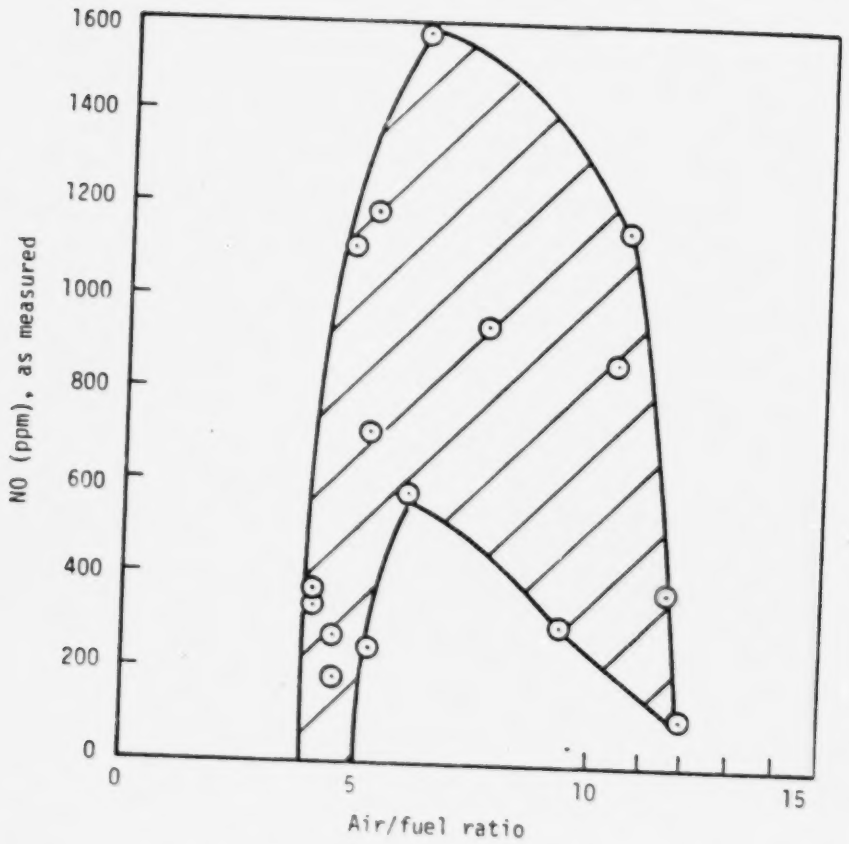


Figure 23. Exit NO concentrations for various air/fuel ratios.

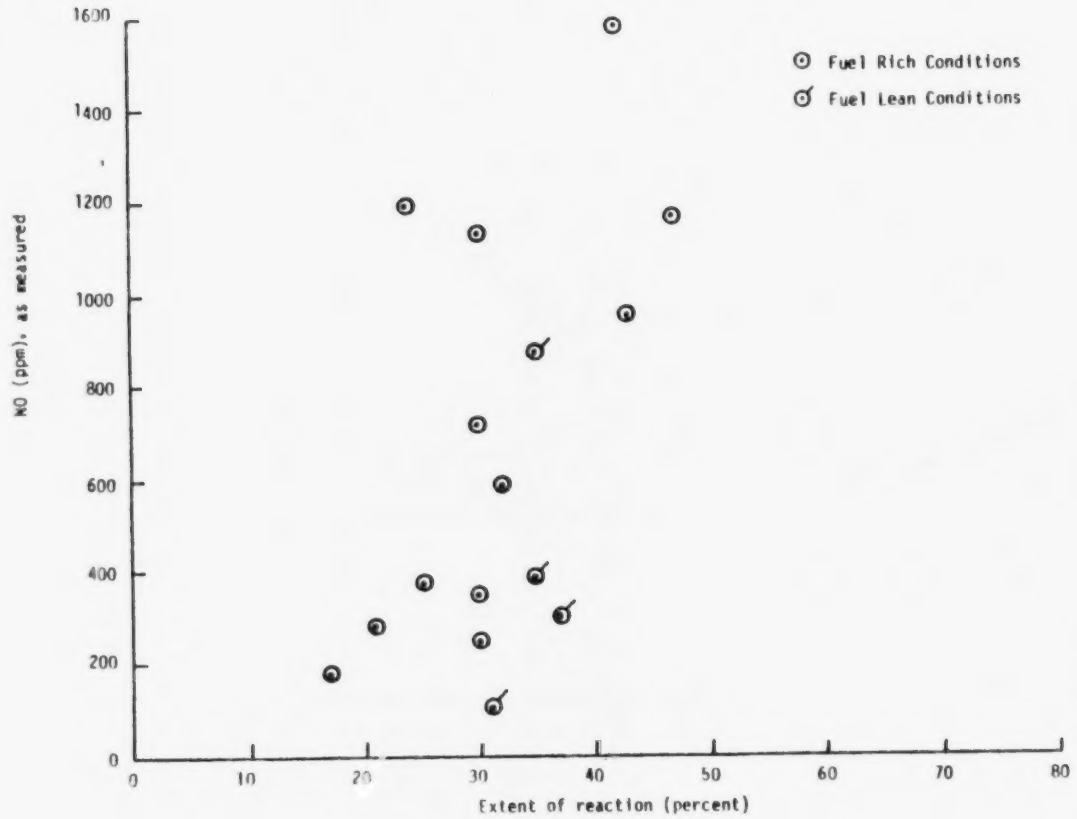


Figure 24. Exit NO concentrations versus extent of coal reaction.

times which, under fuel rich conditions does not allow sufficient time for initially formed NO to decay. From Figure 24 it appears that NO levels are proportional to extent of reaction. Thus, as more fuel is burned higher NO levels will be achieved.

## 3.4 SUMMARY

During the feasibility testing, catalytically aided coal combustion was found to be occurring in the reactor bed as evidenced by bed temperatures higher than exit gas temperatures. For fixed operating conditions, bed temperatures and exit conditions varied with time. The time scale of variation was on the order of minutes. It is hypothesized that degradation of the bed caused by particle deposition was responsible for the changes with time.

Catalyst temperatures up to 1587K (2400°F) were achieved during the tests. Test conditions included equivalence ratios from 0.76 to 2.46 at total flowrates from 30 $m^3$/hr to 58 $m^3$/hr. Preheats, for the most part, were kept within the 603K (625°F) to 616K (650°F) range. Combustion efficiencies were found to be dependent on air/fuel ratio and were estimated to lie between 20 and 70 percent. This range of extent of reaction can probably be associated with coal volatilization. At the temperature levels, heating rates and residence times characteristic of these tests, the primary mechanism of coal consumption is volatilization. Volatilization is very dependent on temperature level and, for the characteristic bed conditions of these tests, extent of reaction can be related to the volatile loss of the coal.

NO emission levels depend on the extent of reaction rising as more coal is consumed. For extent of reactions greater than 40 percent, NO emission levels of 1000 ppm are observed even under overall fuel rich conditions.

The major problem identified by the feasibility testing was the prebed combustion of coal. The occurrence of prebed combustion can lead to bed particle deposition and slagging and causes obscuration of information on the catalytically aided coal combustion process.

Prebed burning develops in the slow moving regions near the reactor walls just upstream of the bed. Ash, exposed as a result of burning in these regions, has a high potential for depositing in the bed thereby plugging the channels near the bed periphery. Once the outer channels plug, the slow moving recirculation zones near the bed periphery grow in size and prebed burning, deposition and plugging accelerate. Eventually, most of the bed becomes clogged and the remaining open channels contribute little to the total heat release. Pressure drop results and post-test visual inspection confirm this hypothesis.

The feasibility tests showed that the combustor system as configured could induce prebed burning. An alteration of the system was necessary to alleviate this problem and permit the evaluation of the burning of coal in a catalytic combustor. The next section describes the evaluation testing system modifications and test results.

# SECTION 4

# EVALUATION TESTING

The feasibility testing showed that the catalytic bed can contribute to coal heat release as evidenced by elevated bed temperatures when compared to exhaust gas temperatures. However, prebed burning of coal and subsequent particle deposition in the bed and eventual bed channel plugging prevented a clear understanding of the process. Therefore, prior to the evaluation testing, the catalytic coal combustor test section design was examined and system modifications were defined to alleviate prebed burning and ash deposition and plugging problems. Without these obscuring effects, the benefits, if any, of burning coal in a catalytic combustor could be evaluated.

The following sections discuss the combustion system modifications and the evaluation test results.

## 4.1 EXPERIMENTAL EQUIPMENT

Figure 25 is a schematic of the new prebed test section design. In this design the previous hot refractory wall prebed test section is replaced by a cool (700K (800°F)) steel wall. This section consists of two concentric steel tubes with the center tube having an ID of 4.8 cm and the outer tube an ID of 8 cm. Thirteen 1.6 cm tubes were positioned axially in the annulus to act as a flow straightener and a heat conduction path from the inside to the outside tube. The potential for coal reaction upstream of the bed is reduced in this system. In addition, the coal/air mixture is present only in the center tube and is shielded from the bed support walls by an equal velocity flow of gas and air in an outer annular section. Thus, the coal/air mixture arrives at the bed with uniform velocity and without ever being in the vicinity of hot walls. This design approach reduces the potential for prebed coal burning and subsequent bed deposition and clogging.

The gas/air mixture in the outer annular flow region can be adjusted during testing to eliminate radial heat flow from the combusting coal mixture. This annular flow then serves the purpose of a wall heat shield as well as a particle mixture wall shield.

Downstream of the annular prebed section and just upstream of the bed a 2.54 cm high 360° quartz window was designed into the test section. Through this window the front of the bed and prebed events could

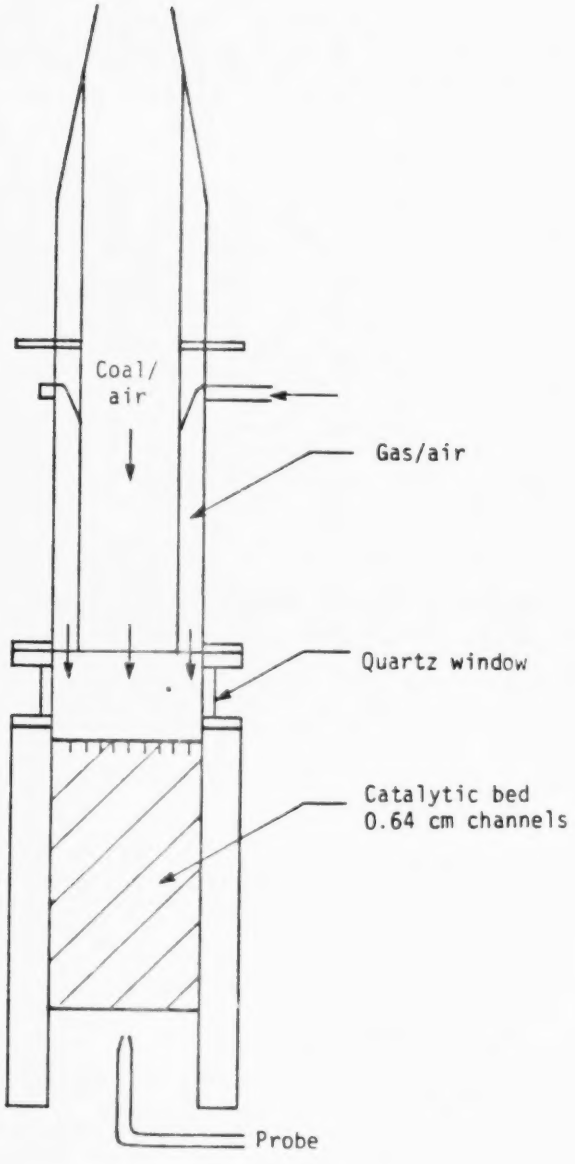


Figure 25. Catalytic coal combustion test section.

be monitored. The outlet of the prebed section was about 7 cm from the top face of the catalytic bed.

The catalyst support section was similar to the test section used in the feasibility experiments. The length of this section was reduced to about 30 cm. With a 17.8 cm long catalyst bed in the section, about 1.9 cm of refractory wall was exposed above the bed. Figure 26 is a photograph of the assembled test system.

### 4.1.1 Catalytic Bed

In the evaluation testing, three catalytic beds were used. One of the beds used a DuPont Torvex alumina support, while the others used Corning Glass Works zirconia spinel. Torvex was used because it has thinner channel webs than zirconia spinel and it has hexagonal channels rather than square channels. It was believed that the thinner webs would reduce the effect of coal slow-down and scattering due to web face impact. Also the low velocity corner zones found for the square cell zirconia spinel beds are not as pronounced in the Torvex hexagonal cell configuration. These Torvex configurational factors should help reduce bed deposition, which was the primary problem encountered during the coal feasibility testing. It should be noted that Torvex is only available in thin sheets and long reactor beds require stacking of sections. This creates alignment and fabrication problems which counterbalance some of the good features of Torvex. Therefore, in addition to Torvex, zirconia spinel catalyst support material was also utilized.

The length of each bed was 17.8 cm. The Torvex bed was composed of seven stacked 2.54 cm sections. The zirconia spinel beds were made from 7.6 cm and 10.2 cm sections. The zirconia spinel had 0.64 cm square cells and the Torvex had 0.64 cm hexagonal cells. The respective void fractions of the zirconia spinel and Torvex beds were 0.6 and 0.8. All beds were coated with Pt and $Co_2O_3$ in nearly similar amounts, as shown in Table 4.

### 4.1.2 Sampling System

The same sampling system described in Section 3.1.3 was used for evaluation testing. The leading edge of the water-cooled probe was located about 6.6 cm below and at the centerline of the back face of the bed. Preliminary tests of the sampling system showed that the gases withdrawn by the probe were from the center section of the catalyst. No traces of gases from the annular section were detected by the probe.

### 4.1.3 Temperature Monitoring

The temperatures in the catalyst bed were monitored by 10 (Pt-Pt Rh 13 percent) thermocouples. The locations of these thermocouples are shown in Figure 27. Half of the thermocouples were located down the centerline of the bed (coal/air side) and the rest were located axially down the outer edge of the bed (propane/air side) 1 cm in from the periphery.

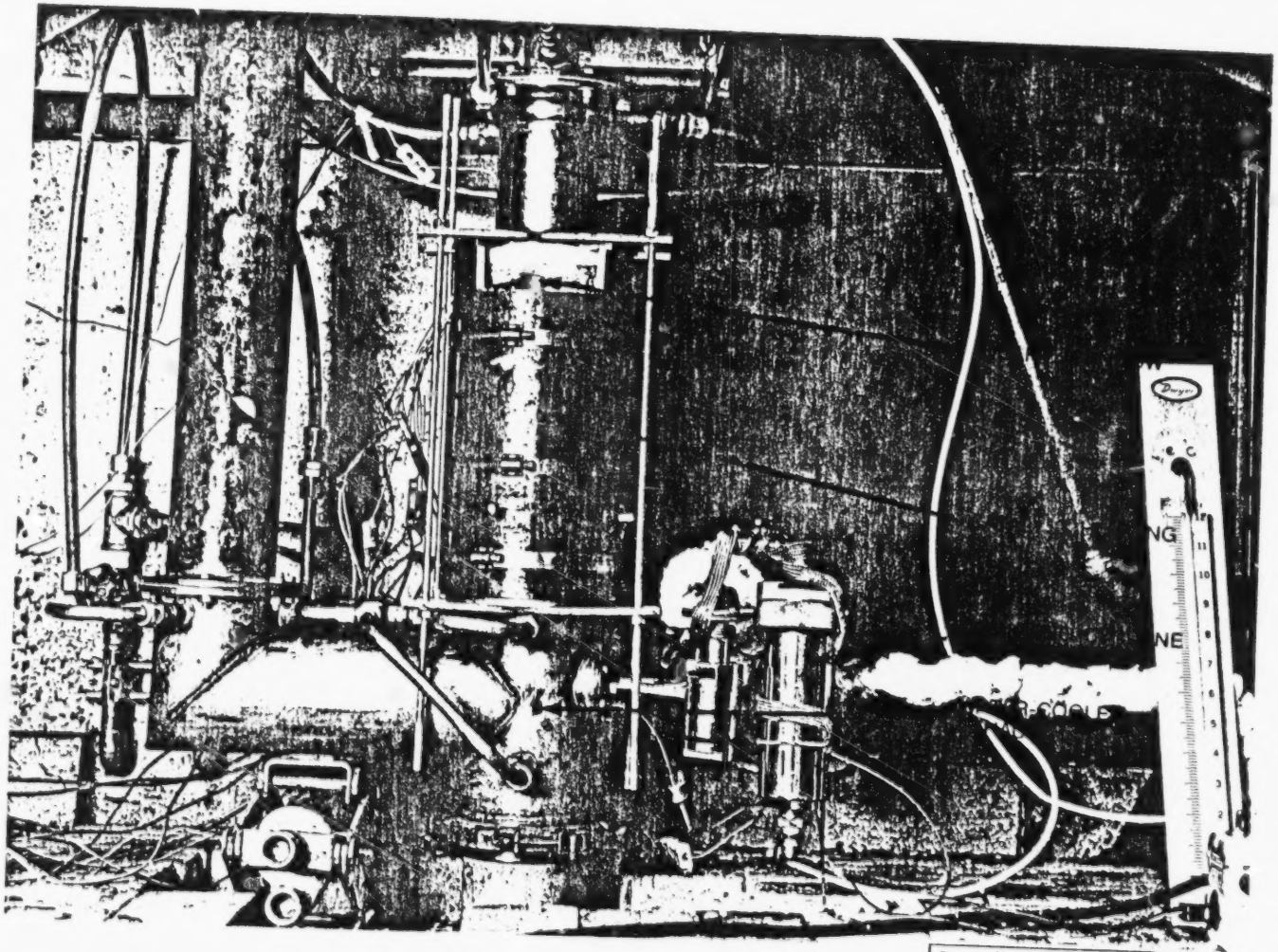

Figure 26. Assembled catalytic coal test system.

Reproduced from best available copy.

TABLE 4. MONOLITH CATALYST COATINGS

| Torvex Bed | | |
|---|---|---|
| Bed Section No. | Wt % $Co_2O_3$ | Wt % Pt |
| 697 (top) | 4.9 | 1.3 |
| 690 | 4.8 | 1.3 |
| 691 | 5.1 | 0.8 |
| 696 | 6.1 | 1.1 |
| 693 | 3.5 | 1.1 |
| 694 | 4.1 | 1.2 |
| 695 (bottom) | 3.7 | 1.2 |

| Zirconia Spinel Beds | | | |
|---|---|---|---|
| Bed Number | Section | Wt % $Co_2O_3$ | Wt % Pt |
| I | top | 4.4 | 0.9 |
| | bottom | 4.3 | 0.9 |
| II | top | 2.8 | 0.8 |
| | bottom | 2.5 | 0.8 |

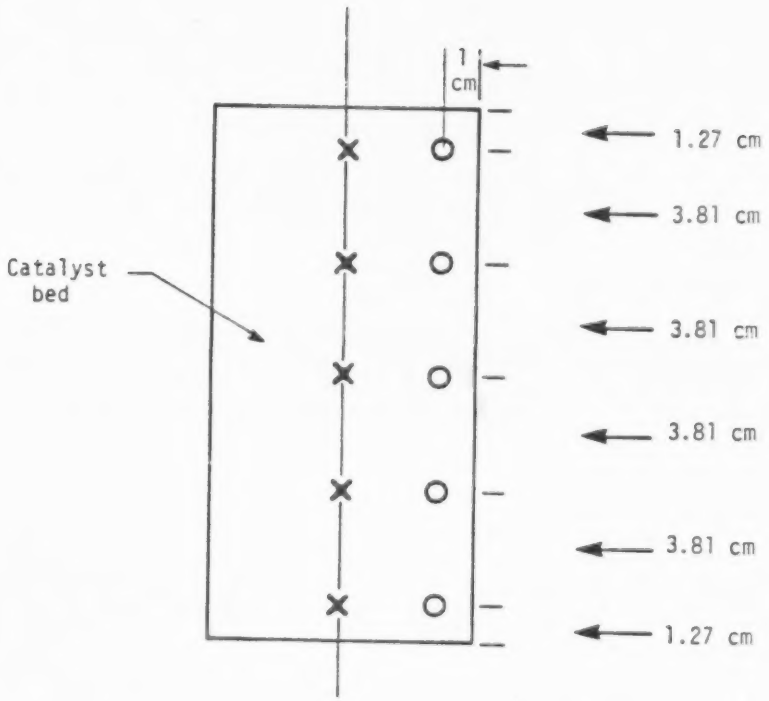


Figure 27. Bed thermocouple locations.

The thermocouples were held in place using refractory cement. The two channels (propane side and coal side) where the thermocouples were positioned were completely sealed at the top and bottom.

During the early tests the bed exhaust temperature was measured by a type K thermocouple positioned on the centerline 7.62 cm below the bed. For later tests, this thermocouple was replaced by a type R thermocouple 2.54 cm below the bed and a type K thermocouple located 10.16 cm below the bed. The two thermocouples were used to monitor any significant post-bed combustion prior to gas sampling.

### 4.1.4 Coal and Feed System

Utah coal was also used in evaluation testing. However, this coal was pulverized to a mean mass size of about 30 with 95 percent passing through 200 mesh. The change to a finer coal was made in an attempt to increase the extent of reaction and reduce coal particle impact and sticking to the front of the bed. Characteristics of this coal are given in Table 1 which is presented in Section 2.

As in the feasibility tests, the coal was fed into the system using the Acrison screw feeder. The maximum usable coal feed rate was about 160 gm/min.

## 4.2 TEST RESULTS

Utilizing the three catalyst beds described in Section 4.1.1, 22 coal combustion test conditions were achieved during the evaluation testing. Data was taken for a range of air preheats, face velocities, and air/fuel ratios. The results are presented in the following sections.

### 4.2.1 Test Procedures

Prior to operation on coal, the bed was self-heated with a propane/air mixture. During this heating the A/F ratios of both the center and annular sections were kept equal. The preheat in the center section was usually maintained at 589K (600°F). The preheat temperature of the annular flow was maintained at 422K (300°F) since annular preheats greater than 422K (300°F) caused flashbacks to occur.

After the bed was heated to 1644K (2500°F), the center propane flow was stopped and the annular propane/air flow and center air flow and preheat were adjusted to the desired values for coal combustion. The annular propane flow was generally maintained at an A/F ratio of 35 to 40.

After the flow adjustments, the front end bed temperature was allowed to drop to temperatures below 644K (700°F). This was done to minimize the sticking of the coal to the front surface of the bed. The coal flow was started at a low rate and gradually increased to the desired value. Final adjustments were then made to the annular flows so as to match the prebed section exit velocities of the annular and center flows and thereby maintain a uniform bed entrance velocity.

Sampling was started a few minutes after final adjustments to the flows and preheat temperatures were made. Sampling was continued for periods ranging from about 10 to 60 minutes. During some of the longer tests, sampling was stopped so that the cyclone particulate catch could be emptied and the downstream filter changed. The reacted coal collected in the cyclone was saved for later ashing to get an indication of extent of reaction. The quantity of sample collected was generally less than 1 gram.

After running tests on coal for approximately one hour, the coal flow was stopped and the combustor was operated entirely on propane and air at specified flow rates and preheat temperatures. Temperature and emissions data were collected at this point to evaluate catalyst degradation through comparison with previous propane combustion data. If significant catalyst degradation had occurred it would be evident in bed temperature and emission level changes.

### 4.2.2 Operating Characteristics

Overall, 22 tests were conducted using the zirconia spinel beds for a combined coal combustion time of about 6.5 hours. Three test conditions were run with the Torvex catalyst bed. However, the data obtained with the Torvex bed was of limited usefulness due to coal feed malfunctions and bed thermocouple failure. Also, during the final test with the Torvex bed, wall temperatures exceeded the material limits and the bed failed thermostructurally. No further tests were run with Torvex beds.

During the evaluation testing of zirconia spinel beds, face velocities were maintained at lower levels than in the feasibility testing. The face velocities ranged from 1.5 m/s to nearly 5.0 m/s and can be roughly grouped into three categories; 1.5, 3.0 and 4.6 m/s. These velocity levels were chosen to increase the residence time and hence the potential for significant heat release in the bed. The tests covered A/F ratios ranging from 3 to 8.2. Air preheat covered the range from 444K to 294K (340 to 70°F). Low preheats were used to avoid coal sticking and buildup on the front of the bed.

As mentioned previously, the front face of the center section of the bed was allowed to cool to about 644K (700°F) before the coal flow was started. Observation through the quartz window upstream of the bed indicated that at temperatures above this level, coal would begin to rapidly accumulate on the front face of the catalyst, causing eventual bridging and blockage of the channels. However, allowing the front section to cool meant allowing the entire bed to cool to some extent. Therefore, maximum back end bed temperatures were usually 1367K to 1533K (2000°F to 2300°F) when coal was introduced.

A typical temperature profile through the bed when operating on coal is presented in Figure 28. As shown, the first several centimeters of the bed remain relatively cool. The temperature slowly begins to increase down the bed with high bed temperatures achieved in the last 3 to 5 centimeters of the bed. This temperature distribution is markedly different from the constant bed temperature case assumed for the analyses described in Section 2. The outer bed temperatures (propane side) generally parallel the inner temperatures. The propane side temperatures

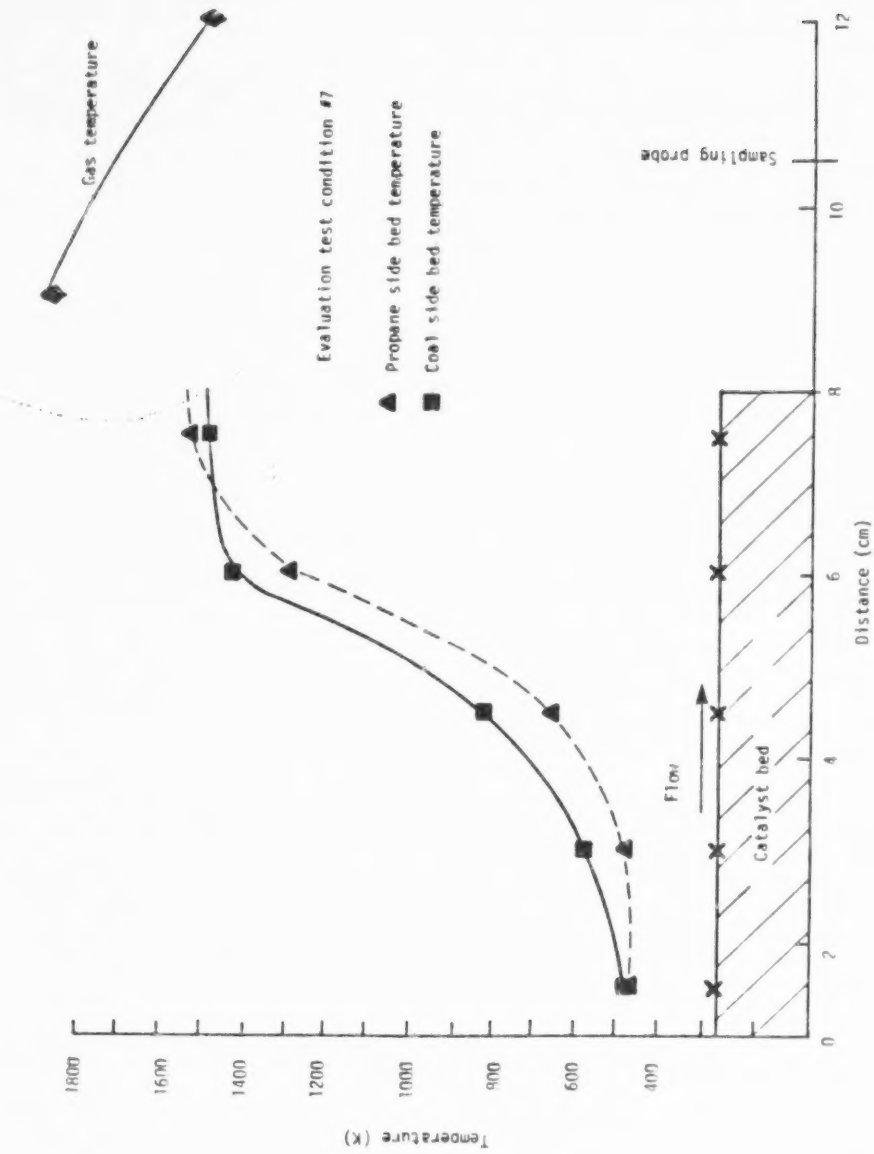


Figure 28. Typical bed and gas temperature distributions during coal combustion.

can be lower or higher than those on the coal side by approximately 60K. Adjustments to the annular propane flow were made during testing to keep temperature differences between these limits.

The data presented in Figure 28 also show that post-bed temperatures can be higher than bed temperatures, particularly at locations 2.54 cm below the bed. It is possible in this case that the partially burnt coal/air mixture is flameholding at the back end of the bed or on the temperature probe, giving the observed high temperature levels. This is in line with the concept that the catalyst bed only initiates the reaction with considerable reaction proceeding downstream of the bed.

As shown in Figure 28, the bed temperature profile indicates that very little heat release occurs in the first few centimeters of the bed. Particle and gas-phase temperatures are also probably low in this initial region. In the last few centimeters of bed length, the bed temperature is high. These high temperatures are a result of either significant heat release in the bed or bed upstream heat conduction from the hot zone downstream of the bed. A combination of these effects probably occurs with the flat portion of the bed temperature curve favoring significant heat release within the last few centimeters of the bed.

To help understand the bed heating process, a simple heat transfer calculation was performed which assumes that convective heat loss to the gas flowing in the channels is proportional to wall temperature. The calculation was one-dimensional along the bed axis and used appropriate gas and solid properties. Figure 29 presents calculated bed temperatures for a variety of gas/wall temperature ratios. Also included on this figure are the measured temperature results taken from Figure 28. In the case where the temperature ratio, Tg/Tw, is unity, no heat is transferred to the gas and wall temperature remains constant. For decreasing temperature ratio, heat loss increases and wall temperature also decreases.

The experimentally determined bed temperatures display two different types of behavior. Near the front of the bed, the bed temperature rises in roughly the manner expected for convective heat transfer to the gas with heat input provided mostly by upstream heat conduction in the bed. However, at roughly 12 cm into the bed the curve rapidly flattens indicating that significant heat release either near the bed surface or in the gas in the channels is maintaining bed temperatures at a nearly constant level. Thus, the end of the bed is acting to initiate combustion which then proceeds downstream of the bed.

When operating on propane, bed temperature profiles differ markedly from the coal cases. Figure 30 gives inner and outer bed surface temperatures when operating on propane. Temperatures both before and after the coal tests are given on this figure. In contrast to the coal results, surface temperatures are fairly high over the full length of the bed with a peak in temperature near the back end of the bed. The overall high bed temperature levels indicate heat is being released near the bed surface, even at the front of the bed. The drop in bed temperature at the back of the bed indicates that heat is being lost from the bed to the

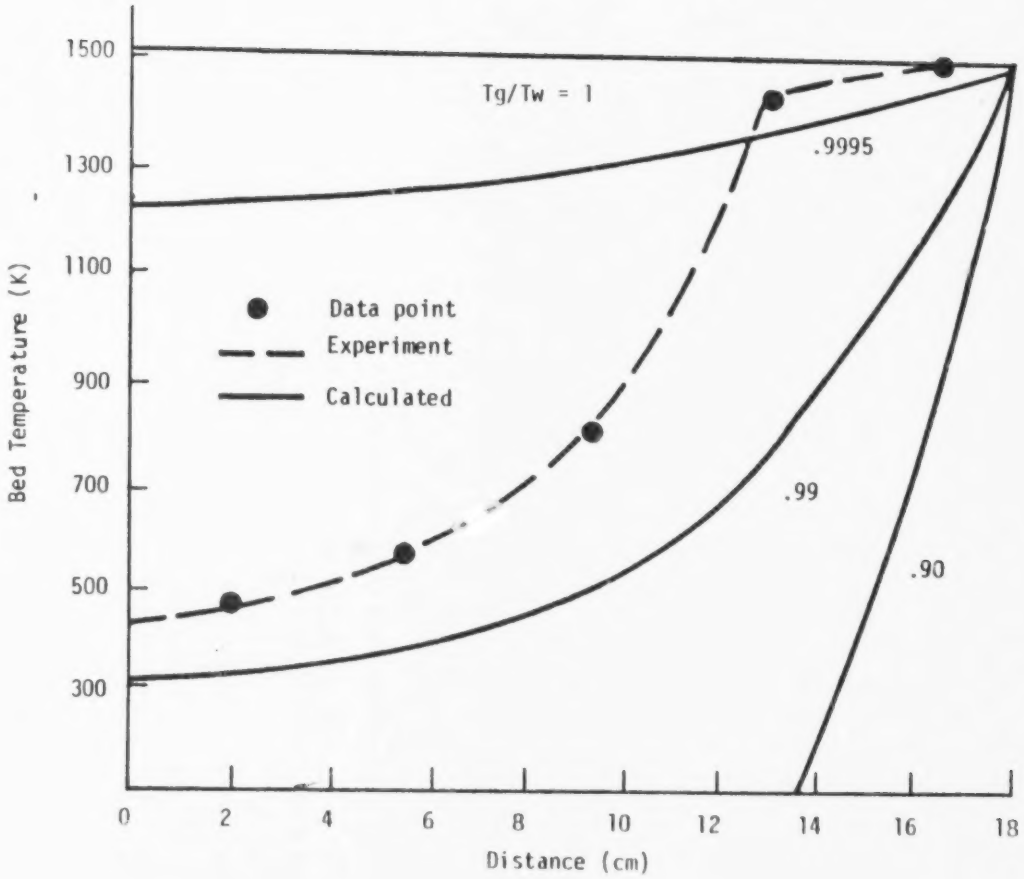


Figure 29. Comparison of measured and predicted bed temperatures.

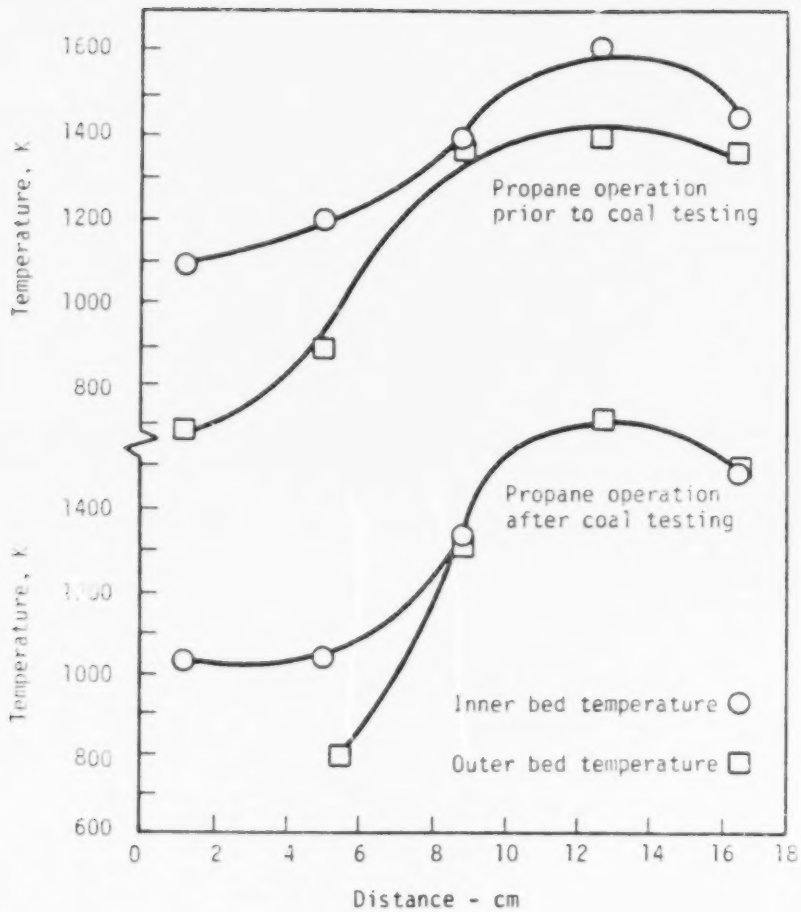


Figure 30. Bed temperature distribution when operating with propane.

downstream region. Thus, with gaseous fuel combustion, heat release is more uniform over the bed length than with solid fuel combustion, and heat is lost to the region downstream of the bed. This difference in behavior is consistent with the difference in fuel characteristics. With coal the fuel has to be volatilized before significant combustion can take place, whereas with propane, the fuel is immediately available, yielding fairly uniform surface combustion over the length of the bed. The coal combustion time scale is longer than the bed residence time and significant combustion occurs in the downstream region. This heat can be transmitted upstream by radiative and conductive heat transfer. When operating the combustor on propane, combustion occurs primarily on the bed surface and heat is lost rather than gained from the region downstream of the bed.

Comparison of propane-fired bed temperatures before and after coal combustion in Figure 30 shows that propane operating characteristics have not changed markedly after firing on coal. Operation on coal consisted of roughly 2 hours of testing which covered A/F ratios from 3 to 8 at a face velocity of approximately 4.6 m/s. Coal testing was terminated when a significant coal deposit was seen to form rapidly on the front of the bed. This deposit was burnt away by operating on propane for a period of about 1.5 hours. The bed temperatures given in the lower part of Figure 30 were then recorded. Thus, the fairly consistent before and after coal combustion bed temperature data presented in Figure 30 represent conditions between which significant coal combustion events took place. It appears that multihour operation on coal and even coal deposition in the bed does not significantly deteriorate bed performance as determined by propane operation. Of course, the propane test may not be at the bed operating limit, either before or after the coal test. For this case, small amounts of bed degradation would not be discernible by these tests. However, it is significant to note that major catalyst degradation, for this and other cases tested, does not occur during coal combustion. The major problem is bed particle deposition which can plug channels and cause testing to be terminated. This occurred several times during the evaluation testing.

Plugging of the catalyst bed is typically preceeded by temperature rises at the front of the bed or major fluctuations in coal feed rate. Rapid plugging usually occurs at the front of the bed, although slow deposition within the bed probably proceeds throughout testing on coal. From visual observation through the prebed quartz window, coal deposition on the front face of the bed webs is seen to be very rapid. Once a small deposit is formed, it rapidly grows within seconds to 1 cm in height, bridges the bed channels and forms a major plug. Some of the coal burns away, but the continual deposition of coal causes a slow growth of the deposit. Deposits 2 to 3 cm in diameter and 1 cm high can easily form in this manner. These deposits are primarily unburned coal since operation on propane at excess air conditions over a period of hours can usually burn away most of the deposits. However, some ash is typically left behind, and ash deposits eventually build up and plug the channels. At this point the bed is inoperative and has to be replaced.

As mentioned above, coal feed rate fluctuations were evident during testing. Careful prebed chamber design could not entirely eliminate the

screw feeder's inherent coal feed fluctuations. The nonsteady nature of the coal combustion process was noted visually in the downstream chamber and a roughly one hertz low level combustion noise was audibly noted during most of the tests.

4.2.3 Test Data

Evaluation test data is summarized in Table 5. The 22 test conditions listed were obtained with two zirconia spinel beds. As mentioned previously, deposition and plugging was still a major problem during this testing. The following paragraphs discuss in chronological order the test events and the bed plugging problems which continually interrupted testing.

At the end of the 1-hour long low face velocity test condition 1, coal deposits rapidly built up on the front of the bed necessitating a switch to propane to burn off the deposits. Having burnt off most of the deposits, the bed was again operated successfully on coal for 1.5 hours at the next two test conditions. Preheat for these test conditions was lowered in an attempt to avoid bed deposition. Upon switching to a higher A/F ratio at test condition 4, a large deposit rapidly built up on the front of the bed, necessitating a switch to propane fuel. It should be noted that test condition 4 was not held for a long period of time and the bed temperatures were much lower than other measured steady operating conditions. Therefore, test condition 4 might not be a valid stable condition but it is included in Table 5 for completeness.

After burning off most of the deposit with propane combustion, the bed was fired on coal at normal preheat and higher face velocity for the next six test conditions for a total run time of approximately 3 hours. All test conditions were steady in time except test conditions 8 and 9, which showed decreasing bed temperatures over test periods of 10 minutes. These conditions are probably not stable. It should be noted that at the end of test condition 9 the bed was operated on propane for roughly 1 hour to burn off a small coal deposit on the front of the bed. Test condition 10 was held for 3/4 of an hour and during that time bed pressure drop rose, indicating substantial bed deposition and plugging. This plugging could not be remedied by operation on propane and the bed was replaced for the following test conditions.

Test conditions 11 through 13 were run at a medium face velocity and normal preheat. This test series lasted for about one half hour and was terminated when a coal deposit built up on the front of the bed. The bed was then run on propane for 1/2 hour to burn up the deposit. At this time it was noted that the back end of the bed had cracked. Therefore, the bed was removed and the cracked area cemented.

Test conditions 14 and 15 were then run on coal for a test time of 20 minutes. Testing was terminated when deposits clogged the bed. Operation on propane helped burn off some deposits. However, mechanical cleaning and recatalyzing of the bed were needed to restore the bed to operable condition for coal firing. Test conditions 16 through 18 were then run on coal for a test time of over 1/2 hour. Test conditions 16 and

TABLE 5. EVALUATION TEST DATA SUMMARY

| Test No. | A/F | Face Velocity m/s | Preheat Temp K | Back End Bed Temperature | | Gas Temperature | | | Exhaust Gas Composition | | |
|---|---|---|---|---|---|---|---|---|---|---|---|
| | | | | | | Distance From Bed | | | | | |
| | | | | Inside K | Outside K | 2.5 cm K | 6.6 cm K | 10.2 cm K | $O_2$ % | $CO_2$ % | NO ppm |
| 1 | 4.6 | 2.7 | 444 | 1506 | 1478 | -- | 1367 | -- | 8.9 | 9.5 | 808 |
| 2 | 4.3 | 1.8 | 322 | 1313 | 1338 | -- | 1403 | -- | 3.3 | 13.3 | 1160 |
| 3 | 3.0 | 1.6 | 294 | 1314 | 1269 | -- | 1499 | -- | 1.4 | 12.1 | 880 |
| 4 | 5.2 | 1.6 | 294 | 1089 | 978 | -- | 1317 | -- | 14.0 | 5.7 | 466 |
| 5 | 6.3 | 4.6 | 467 | 1621 | 1660 | 1638 | -- | 1441 | 0.5 | 15.0 | 1630 |
| 6 | 5.2 | 4.5 | 456 | 1632 | 1673 | 1631 | -- | 1458 | 0.6 | 12.0 | 1200 |
| 7 | 3.0 | 4.3 | 439 | 1468 | 1521 | 1867 | -- | 1502 | 1.2 | 9.7 | 775 |
| 8 | 8.2 | 4.7 | 475 | 1200 | 1244 | 1522 | -- | 1311 | 1.1 | 13.5 | 1125 |
| 9 | 6.7 | 4.6 | 467 | 1217 | 1239 | 1683 | -- | 1444 | 5.0 | 13.0 | 1450 |
| 10 | 3.0 | 5.0 | 508 | 1458 | 1552 | 1922 | -- | 1514 | 1.9 | 9.5 | 650 |
| 11 | 4.7 | 3.1 | 462 | 1808 | 1747 | 1831 | -- | 1381 | 0.5 | 13.0 | 1100 |
| 12 | 3.9 | 3.1 | 463 | 1706 | 1717 | 1806 | -- | 1390 | 0.8 | 11.5 | 700 |
| 13 | 3.3 | 3.1 | 468 | 1664 | 1714 | 1794 | -- | 1451 | 1.1 | 11.0 | 350 |
| 14 | 3.0 | 3.0 | 455 | 1511 | 1607 | 1723 | -- | 1373 | 1.2 | 9.2 | 700 |
| 15 | 2.6 | 3.0 | 489 | 1467 | 1544 | 1733 | -- | 1422 | 0.5 | 13.0 | 750 |
| 16 | 4.7 | 3.1 | 467 | 1617 | 1678 | 1772 | -- | 1288 | 3.3 | 11.7 | 852 |
| 17 | 5.9 | 3.1 | 469 | 1628 | 1639 | 1709 | -- | 1267 | 0.4 | 13.8 | 885 |
| 18 | 8.0 | 3.2 | 474 | -- | -- | -- | -- | -- | -- | 11.0 | 753 |
| 19 | 5.3 | 3.0 | 367 | -- | -- | -- | -- | -- | -- | -- | -- |
| 20 | 3.4 | 1.7 | 360 | 1478 | 1561 | 1661 | -- | -- | 0.9 | 13.8 | 874 |
| 21 | 4.6 | 1.6 | 325 | 1381 | 1456 | 1553 | -- | -- | 2.0 | 14.7 | 875 |
| 22 | 5.9 | 1.6 | 325 | 1308 | 1367 | 1428 | -- | -- | 4.5 | 13.5 | 793 |

17 were stable with test condition 18 exhibiting a drop of bed temperatures with time and significant bed deposition. Therefore, test condition 18 is probably not stable. After burning off the deposit with propane, coal was fired at the medium velocity and lower preheat at test condition 19. Bed temperatures began to drop at this condition, indicating a probable unstable condition. Test conditions were then changed to the lower velocity and preheat case and test conditions 20 through 22 were recorded over a period of 1/2 hour. These were stable test conditions which were interrupted once by deposition problems and subsequent bed cleaning by propane combustion. Tests were finally terminated at the conclusion of test condition 22 when deposits permanently clogged the bed, rendering it inoperable on coal.

These brief comments on the test events indicate that deposition was a continuing problem which interrupted testing and altered bed operating characteristics between bed deposition cleaning cycles. Thus, the data obtained is for beds which are constantly altered by bed deposition and eventually, bed replacement. Hence, considerable scatter in the data was expected and will be evident in Table 5 and the figures which present this data.

Figure 31 gives the extent of reaction as calculated from exit gas composition data and ash tests of the partially burnt coal collected in the probe. These evaluation test results represent stable operating conditions at 1.5, 3.0, and 4.6 m/s face velocities and preheat temperatures of 294K to 509K (70°F to 455°F). It should be noted that preheats were held to this level to prevent coal sticking and deposition at the front of the bed. For the most part 1.5, 3.0 and 4.6 m/s face velocity conditions were set at about 294K and 466K (70°F and 380°F) preheats respectively.

Also included on Figure 31 is a curve of the theoretical combustion limit based on the available oxygen. The extent of reaction results based on gas composition, though exhibiting some scatter, fall near the theoretical combustion curve. This shows that, under fuel rich conditions, the combustor has consumed most of the available oxygen and significant heat release has occurred.

The much higher and nearly uniform extent of reaction results based on the ash tests indicates that almost total coal devolatilization has taken place. On the order of 60 percent total coal devolatilization can be reasonably expected for this coal type and heating rate. At the air/fuel ratios, heating rates, residence times and maximum bed temperatures found for these cases, significant heterogeneous combustion of the coal is probably not expected. This is in agreement with the Section 2 analysis results which show the major coal consumption mechanism at low air/fuel ratios is by volatilization. Therefore, the total weight loss of the coal can be primarily associated with volatilization.

To help define the coal reaction mechanism, Scanning Electron Micrographs (SEM) were taken of reacted and unreacted Utah coal samples. Figures 32a and 32b shows the raw coal at magnifications of 200x and 1000x. Figures 32c and 32d show the reacted coal at magnifications of

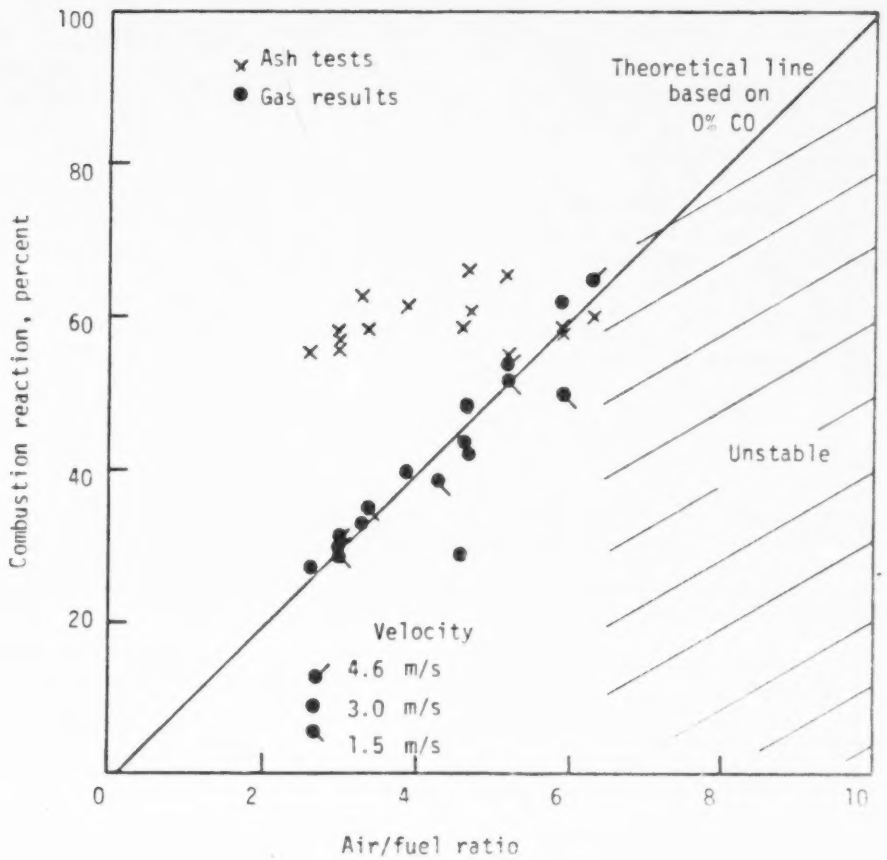


Figure 31. Extent of coal reaction with air/fuel ratio.

(a) Utah coal as received, 200x magnification.

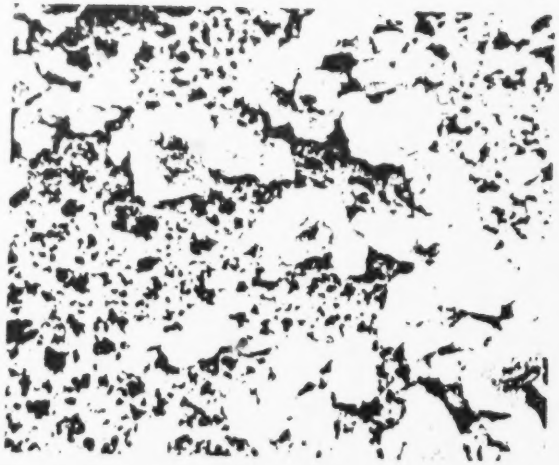

(b) Utah coal as received, 1000x magnification.

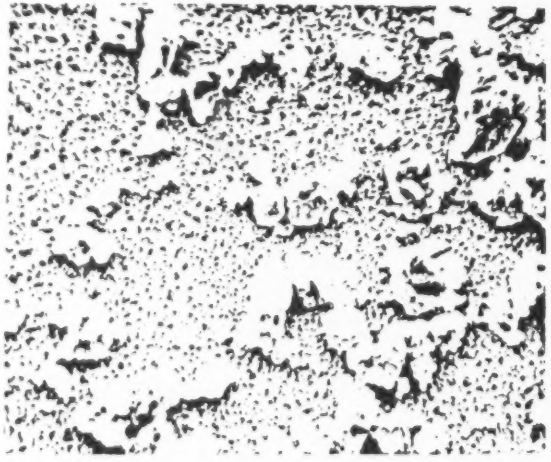

(c) Utah coal after combustion, 200x magnification.

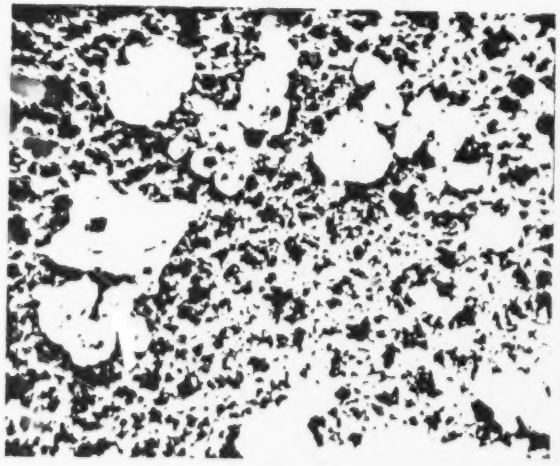

(d) Utah coal after combustion, 1000x magnification.

Figure 32. SEM photomicrographs of unreacted and reacted Utah coal samples.

200x and 1000x. By comparison, it appears as if the size of the reacted particles has increased after passing through the reactor, due to swelling. The size change observed in Figure 32a versus 32c is probably obscured by particle agglomeration. However, comparing Figures 32b and 32d shows a definite increase in particle size of possibly 10 percent or more through the reactor. Figure 32d shows evidence of cenosphere formation and the sharp angular edges observed in Figure 32b have been rounded. There appear to be large holes in some of the smaller particles, which might be attributed to rapid particle volatilization while the coal is in a softened state. These photographs show that the basic coal matrix has not been fully burned away, supporting the hypothesis that the primary consumption of the coal particle is probably through volatilization.

The difference between the gas composition and ash reaction results shown in Figure 31, is a measure of how much unburned fuel exits the combustor. It should be noted that the extent of reaction based on gas composition allowed for the formation of CO. Thus, the extent of reaction values already include some amount of unburned fuel in the form of CO.

The convergence of the gas composition and ash results at an air/fuel ratio of 6 indicates that all the fuel available from the coal has been combusted. This air/fuel ratio corresponds roughly with stoichiometric conditions for the volatiles only. Above an air/fuel ratio of roughly 6.3, steady coal combustion could not be achieved and bed temperatures were observed to drop with time. As the air/fuel ratio increases beyond 6, the combustion becomes fuel lean relative to the volatiles. The extra thermal mass of the lean mixture may be preventing ignition from being maintained and the combustion process degenerates. From the analysis, as the air/fuel ratio rises much above 6 the bed and gas temperature both peak and then begin to fall. Thus, above an air/fuel ratio of 6, thermal mass considerations lead to lowered temperatures which can eventually lead to a noncombusting condition.

The effect of face velocity on extent of reaction is seen to be fairly small at low air/fuel ratios, but more significant at higher air/fuel ratios. Extent of reaction appears to increase with velocity at high air/fuel ratios. It is possible that the higher velocities increase the mass and heat transfer between the gases and the bed surface, thereby promoting a greater extent of reaction of the mixture.

Figure 33 gives the variation of bed temperature with air/fuel ratio. As previously mentioned, significant bed particle deposition occurred between tests on several occasions. Thus test results are expected to exhibit scatter if plotted as a single line. Therefore, the data points in Figure 33 were connected by lines which represent groups of conditions taken with a single bed of unaltered form. For identical conditions, trends between these lines should be similar.

The results in Figure 33 show that bed temperatures increase with air/fuel ratio for bed velocities of 3.0 and 4.6 m/s. Also, in two cases a flattening of temperature rise with air/fuel ratio was noted. In contrast to this behavior, a test series at a face velocity of 1.5 m/s showed that bed temperature decreased with air/fuel ratio. However,

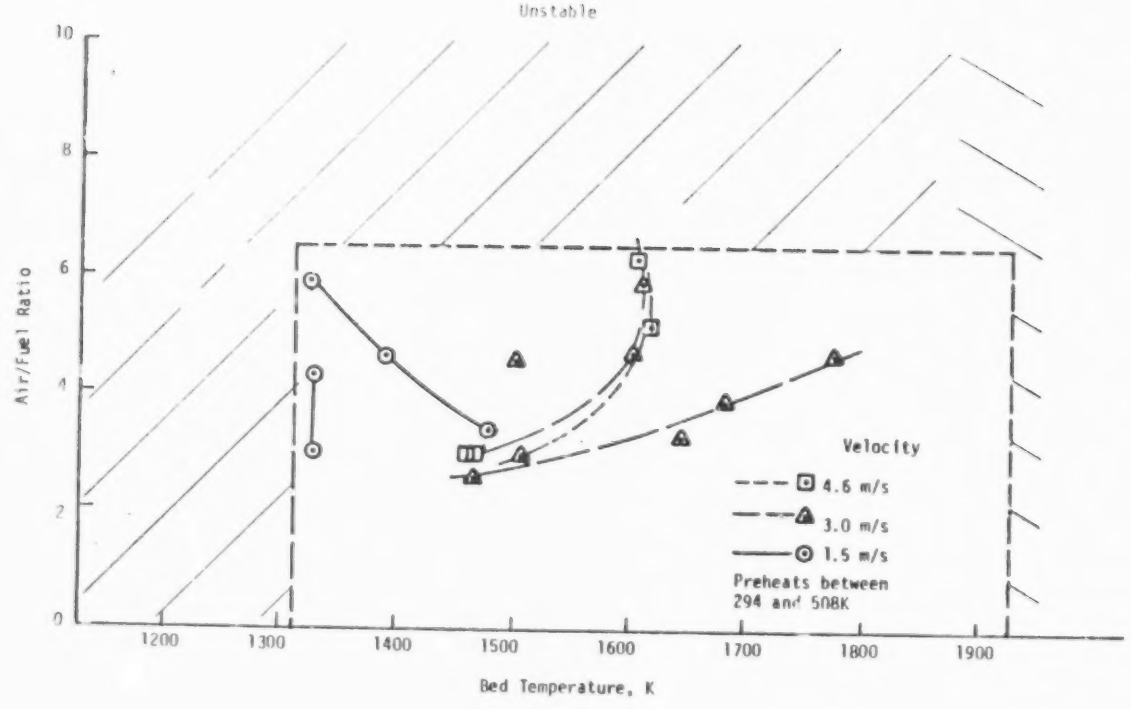


Figure 33. Bed temperature variation with air/fuel ratio.

another test series at this same condition showed no change in bed temperature with air/fuel ratio. The lack of consistency in data trends at a face velocity of 1.5 m/s does not permit any firm conclusions to be reached on this data.

The increase in temperature with air/fuel ratio at face velocities of 3.0 and 4.6 m/s is consistent with the extent of reaction results presented earlier, in that as air/fuel ratio increases, extent of reaction, combustion heat release and bed temperature increases. As the air/fuel ratio increases beyond 6, all the volatiles are burned and the combustion becomes nonsteady as discussed previously.

In addition to the air/fuel ratio operating limit, it appears that there is a lower bed temperature limit below which combustion cannot be sustained. For these tests the lower limit was found to be roughly 1311K (1900°F). As temperatures drop below this value, the strongly temperature dependent volatilization processes slow down significantly, and for system characteristic residence times the amount of volatiles released cannot sustain the process.

The third limit constraining the operating range of the bed is the upper temperature limit of the bed materials. This is set at 1922K (3000°F) in Figure 33. As better materials become available, this limit will be shifted to higher temperatures. However, the best presently available materials should not be operated much above this temperature limit.

From Figure 33 it can be seen that material and stable operating bounds limit the combustion process to only rich operation at air/fuel ratios below roughly 6.3 (or equivalence ratios greater than 1.6) and temperatures between roughly 1311K (1900°F) and 1922K (3000°F). System limitations prevented operation at air/fuel ratios below 2. It is very possible that a lower operating bound on air/fuel ratio also exists. This is supported somewhat by the model predictions in Section 2 which show a drop in bed temperature as air/fuel ratio is decreased. In conclusion, operating bounds for coal burning in a catalytic combustor are fairly narrow for the velocities, preheat temperatures, and bed geometries investigated.

It should be noted that the Section 2 analysis is consistent with the test results only in terms of data trends. Values of temperatures, extent of reaction, etc. are not adequately quantitatively predicted by the model. This is probably a result of the failure of some of the basic simplifying assumptions of the model.

A fundamental assumption of the model is that bed temperatures are uniform over the combustor length. As shown in Figure 28, experimentally found bed temperatures start at very low levels near the front of the bed and increase to high levels near the back end. For short beds this temperature gradient significantly violates the constant temperature assumption of the model and leads to differences between data and predictions. Perhaps for longer beds, the temperatures would be more uniform over the full length of the bed and analysis and experiment would exhibit better agreement.

Another major assumption of the model is initial uniform particle size rather than the polysized distribution of the actual coal supply. As mentioned in the analysis section, small coal particles are consumed much more rapidly than larger particles. With a polysized distribution, the small particles will initiate combustion and help heat the larger particles. Thus, with a polysized distribution it is expected that combustion will occur over a larger distance and over a wider range of operating conditions than is possible for a single coal particle size. The monosized coal particle assumption of the model can yield results quite different from the polysized coal experiments.

Heat loss is another factor not adequately accounted for in the model. Due to coal sticking and deposition problems the prebed combustor section for the evaluation testing was modified to operate at low temperature. Also, a quartz window was factored into the design to permit visual observation of prebed events. These modifications produced a considerable heat loss which is not accounted for in the nearly adiabatic analytical model.

In addition to these major assumptions, there are also several minor assumptions in the model which can impact the comparison between predictions and data. It is obvious from these brief comments that the analytical model requires significant improvements before adequate quantitative predictions can be made. However, bed deposition problems can alter bed operating characteristics in a manner which cannot be reasonably modeled. Therefore, the best that can be hoped for is a qualitative model prediction which is the type of prediction the current analytical technique provides.

Figure 34 presents the combustor NO emissions as a function of air/fuel ratio. The data, for the most part, shows that NO increases with air/fuel ratio for all face velocities. This is reasonable since as air/fuel ratio increases the amount of oxygen available to the volatile fuel nitrogen increases. As is well known, the presence of oxygen leads to significant amounts of NO formation from the volatile fuel nitrogen. The levels of NO are quite high, achieving maximum levels of over 1600 ppm even at equivalence ratios of around 1.6. Typically, when a conventional coal combustor is operated at these rich equivalence ratios NO levels are much reduced from the levels observed in this study. However, these combustors operate at fairly long residence times, on the order of one second, compared to the short residence times of order 0.01 second of this study. At these short residence times we are observing the early events during coal combustion.

Even for very low levels of air, the nitrogen volatiles which first come off the coal enter an environment which has an abundance of available oxygen. These nitrogen volatiles then have a high potential for conversion to NO. As further volatilization and combustion take place, oxygen becomes depleted and eventually the mixture becomes oxygen deficient. By this time significant NO has already formed and high levels can be measured. Given sufficient time under oxygen deficient conditions this "early NO" can be reduced to low levels. However, in this study insufficient residence time is available in the combustor to reduce the NO

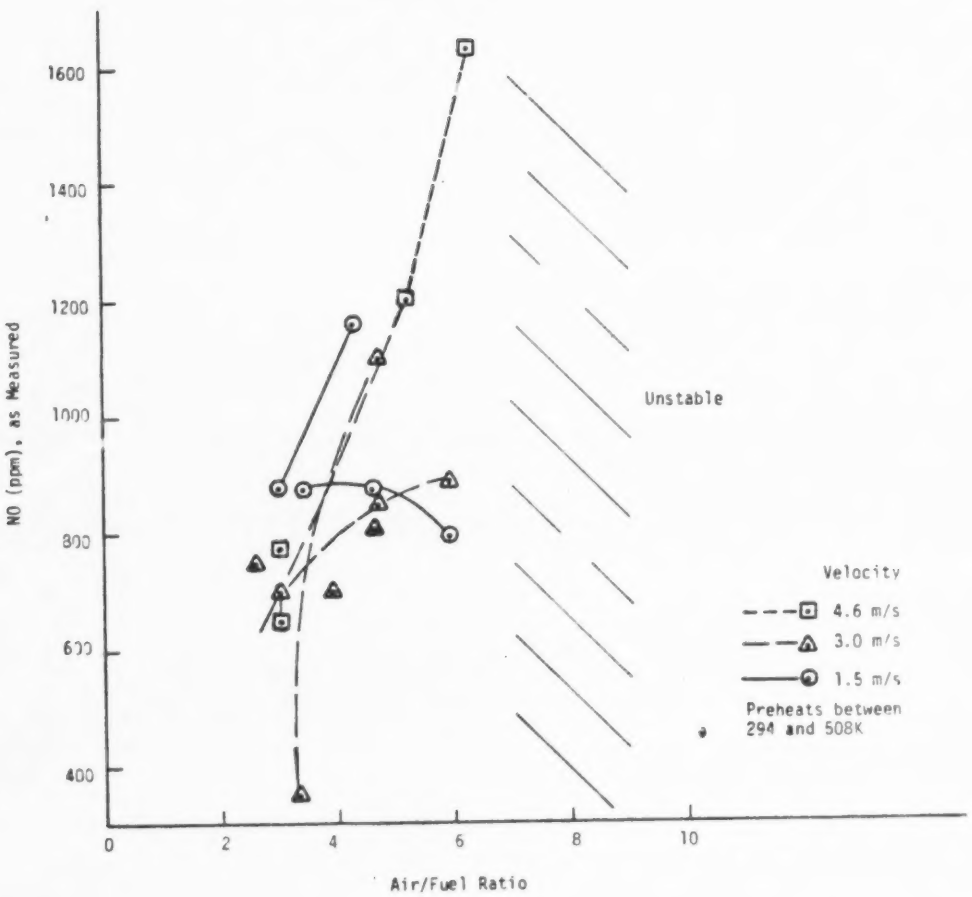


Figure 34. Measured exit NO variation with air/fuel ratio.

and therefore high levels are observed. At air/fuel ratios greater than 5, Figure 34 shows that NO levels decrease with decreases in velocity or increases in residence time which is consistent with the above conjecture. However, at lower air/fuel ratios the 1.5 m/sec velocity case exhibits higher levels than expected based on residence time considerations. The reason for this is not clear.

Even though the NO levels are high, it should be noted that conversions of fuel nitrogen volatiles to NO is fairly low, being 20 to 40 percent of the maximum theoretical conversion possible. These conversions were calculated considering the fraction of coal that is burned and assuming that, in the theoretical case, all of the oxygen needed to form NO is available.

Figure 35 gives the variation of NO with bed temperature. These results, which span the air/fuel ratio range from 2.6 to 6.3 and velocities from 1.5 to 4.6 m/sec, show that at fixed velocity, NO increases with temperature. This is expected on two accounts. First, local temperatures can be higher than bed temperature and thermal NO formation might be enhanced by increased bed temperature. Second, increased temperature is evidence of increased burning due to more available oxygen which means that more fuel nitrogen volatiles have the potential for being oxidized. The major effect observed in Figure 35 is probably due more to the increase of air/fuel ratio than the effect of temperature by itself on NO.

In conclusion, even at low air/fuel ratios, high levels of NO are found for coal burning in a catalytic combustor. This is primarily a result of the early NO not being reduced under rich conditions due to insufficient residence time.

### 4.2.4 Comparison with Conventional Combustion

In comparing the burning of coal in a catalytic combustor with conventional coal combustion, the problem of bed deposition and plugging stands out. In conventional coal combustion solid surfaces in the presence of burning coal are avoided. Conventional burner coal spreaders or impellers do come into contact with the coal stream and are susceptible to erosion and blockage problems. However, the coal stream is cool at the impeller or spreader and the problem of deposition is thereby minimized. In the burning of coal in a catalytic combustor the bed surfaces are in the presence of coal particles at various states of combustion. With this type of environment it is very probable that bed deposition and blockage will occur. Any advantages of burning coal in a catalytic combustor are strongly offset by the major problem of bed deposition and blockage.

Gas- and oil-fired catalytic combustors are capable of very large volumetric heat release rates, on the order of $5 \times 10^6$ J/hr-Pa-m$^3$. During the tests on coal the catalytic combustor achieved heat release rates up to about $2.0 \times 10^5$ J/hr-Pa-m$^3$, which is an order of magnitude lower than gas- and oil-fired catalytic combustors but is an order of magnitude greater than typical coal-fired combustion system values. These values are only for the volatile fraction burned. Complete burnout

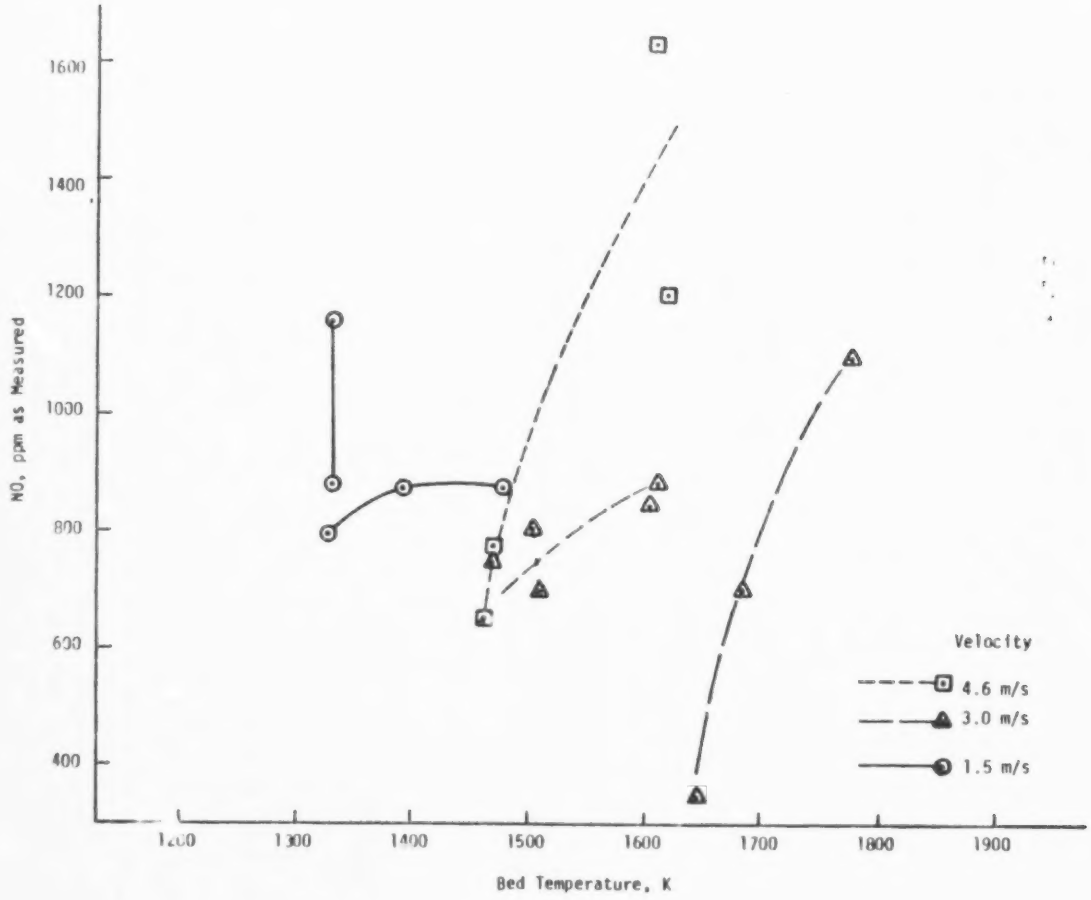


Figure 35. Measured exit NO variation with bed temperature.

requires greater combustor volume. These high heat release rates indicate that burner size can be advantageously reduced from conventional practice.

It should be noted that the high volumetric heat release rate is a result of the presence of the bed as well as the premixed nature of the fuel and air. Csaba (reported in Reference 5) measured the flow speed required to keep a premixed coal/air flame stationary in an empty diverging insulated duct. The maximum achievable flow velocity at conditions characteristic of the catalytic combustor tests was found to be 1.2 m/s. Velocities higher than this will blow the flame down the empty duct. At these same conditions the catalytic combustor operates stably at a velocity of 3 m/s.* Thus, the catalytic combustor is able to consume fuel at 2.5 times the rate of a conventional combustor given the same air/fuel mixture. This increase in heat release rate is due to two factors. First, the monolith bed acts as an upstream heat path to promote heating of gas and particles and eventually ignition of the particles. Second, catalytic reactions on the surface help initiate reaction and generate heat which then speeds up the reaction of the particles in the gas stream. The degree to which each of these mechanisms participate is not known. However, their presence has been confirmed by the results of this study.

Another benefit of the catalytic combustor system might be the stability of combustion achieved at very low air/fuel ratios. Tests showed that stable combustion and nearly full volatilization of the coal could be achieved at air/fuel ratios which only represent 26 percent of the air needed for complete combustion. The catalytic combustor might be useful as a very rich combustion flameholder downstream of which the secondary air mixing could be optimized for $NO_x$ control rather than for stability.

One of the primary advantages of gas- and clean oil-fired catalytic combustors is their low temperature operating capability. This characteristic can be beneficially applied to reduce thermal $NO_x$ emissions which are very temperature dependent. However, for coals or heavy oils which have a significant amount of nitrogen bound with the fuel, temperature does not significantly impact the formation of fuel NO which is the dominant source of NO for these fuels. Therefore, catalytic combustor temperature control does not appear to offer much of a benefit in terms of significantly reducing NO emissions. In fact, the high NO emissions measured during the testing confirms that short residence time premixed burning, such as that achieved in the catalytic combustor, can yield very high NO levels even under fuel rich conditions. A long residence time downstream chamber is needed to reduce NO levels to those achieved by conventional diffusion type coal-fired low $NO_x$ burners.

In conclusion, the catalytic combustor offers some advantages over conventional combustors in heat release rate and possibly in low air/fuel

---

*It should be noted that this velocity is below the coal/air mixture transport velocity.

ratio combustion stability. These characteristics might be beneficially applied to a very rich flame holder concept in which downstream mixing could be optimized for NO control with a lesser emphasis on stability requirements. In order to apply these potential benefits the major problems of particle deposition and plugging in the bed must be overcome.

## SECTION 5

## CONCLUSIONS AND RECOMMENDATIONS

The results of this study show that pulverized coal can be burned in a catalytic combustor. Pulverized coal combustion in catalytic beds is markedly different from gaseous fuel combustion. Gas combustion gives uniform bed temperatures and reaction rates over the entire bed length and, depending on flow conditions and bed geometry, little combustion may occur downstream of the bed. For the bed configurations, fuel supplies, and test conditions studied, pulverized coal combustion results in significant temperature and reaction gradients over the bed length and substantial combustion downstream of the bed. Thus, for pulverized coal combustion, the bed acts mainly as an initiator and stabilizer of combustion. A significant portion of the combustion process, primarily that associated with char burnout, occurs downstream of the bed.

Test results show that the coal was substantially devolatilized by the combustor for all air/fuel ratios tested. Exit gas composition results show that the extent of reaction of the coal is near the theoretical limit, given the available oxygen. Increased bed velocity brings the extent of reaction closer to the theoretical limit.

Catalytic bed operating limits are bounded by bed material upper temperature limits, lower temperature volatilization limits, thermal mass air/fuel ratio limits and particle deposition preheat limits. Presently available bed materials limit the maximum bed operating temperature to 1900K. Based on the lower temperature results of this study and known relationships between temperature and coal volatilization histories, it appears that 1300K is the minimum bed operating temperature needed to sustain steady combustion. Above an air/fuel ratio of 6.0, bed temperatures decrease with time. This air/fuel ratio roughly corresponds with the stoichiometric air needs for only the coal volatiles. Increases of air flow above this level probably yield thermal mass loads too high for maintenance of steady state combustion conditions.

Front end bed and air preheat temperatures must be less than 500K to avoid coal deposition on the front of the bed. Above 500K char deposits rapidly build up on the front of the bed and plug channels. These deposits can be burned off by operating the bed on propane fuel under excess air conditions. However, after several bed cleaning cycles, sufficient ash builds up to plug bed channels. This deposition of char and ash in the bed was the major problem identified in burning pulverized coal in a catalytic combustor. Therefore, low air preheat temperatures

and cooled prebed sections which prevent prebed combustion are required to reduce the potential for bed char deposition. During this study bed channel plugging reduced the useful life of the beds to about 6 hours.

Degradation of the catalyst by chemical attack was not as severe a problem as deposition This was confirmed by propane tests before and after coal combustio.. These tests showed that previously attained gas combustion conditions could be nearly duplicated following a significant amount of coal combustion testing.

Comparison of catalytic coal combustion with conventional premixed coal combustion indicates that the presence of the catalytic bed significantly improves system volumetric heat release based on volatiles. This characteristic of the catalytic combustor could be beneficially used to reduce combustor size for a given volatiles heat release. As indicated previously, coal combustion is only initiated in the limited lengths of the catalytic combustors tested. Therefore, provision for downstream of bed coal burnout must be incorporated into any system design. This additional coal burnout volume will be a significant fraction of the total combustion volume.

NO emissions for the catalytic combustor are high even under fuel rich conditions. The NO formed early under locally lean conditions does not have sufficient time within the combustor to decay under oxygen deficient conditions. No clear trend of NO emissions with extent of prebed combustion could be observed from the data. The effect of the extent of combustion before the bed versus combustion within the bed is within the fairly large data scatter for these tests. Subsequent stages with longer residence times are needed to decay NO concentrations to low levels. As expected, NO levels increase with air/fuel ratio and decrease with increases in residence time.

As indicated previously, the coal-fired catalytic combustor may have some benefit as a high heat release rate, very fuel rich, initial flameholder which is followed by a non-catalytic coal burnout section. This type of system could have heat release, stability and emission benefits. However, for this system to be viable the bed deposition and channel plugging problems must be solved. Recommendations to help solve these problems include:

- Use of microsized coal supplies ( ~1 μsize range) to minimize bed face impact and sticking. The smaller particles would tend to follow gas streamlines and thereby avoid impacts with solid surfaces over which the gas is flowing. Coal supplies could also be blended with oils to widen the operating range of the system. The coal could be ground with the oil and fed into the system as a slurry. This would eliminate grinding and feed problems associated with particles of this size range.

- Employ longer beds with actively cooled front sections to minimize front end deposition. With a longer bed the front end could remain cool while the back end is hot for a considerable distance. This should improve extent of reaction and stability characteristics.

- Use of thin webbed beds to minimize bed front surface area off of which coal can be scattered. Also, use round channels to minimize slow moving zones where coal particles can burn and then stick to adjacent surfaces.

Taking these steps might improve operating characteristics and deposition problems considerably. Once this problem is alleviated, a more extensive test program could be undertaken to make a more complete assessment of the performance and emissions benefits of burning coal in a catalytic combustor. For example, complete test systems could be constructed which would consist of a rich burn catalytic flameholder, similar to those tested herein, plus a conventional burnout section in which additional combustion air is added and heat is extracted. Results achieved with this system could then be compared to existing staged and unstaged premixed pulverized coal results and conventional diffusion flame pulverized coal burners to determine more completely the performance and emissions benefits, if any, of this type of system.

## REFERENCES


1. Kesselring, J. P., et al., "Design Criteria for Stationary Source Catalytic Combustion Systems," United States Environmental Protection Agency Report EPA-600/7-79-181, August 1979.

2. Annanalai, K. and Durbetaki, P., "A Theory on Transition of Ignition Phase of Coal Particles," Combustion and Flame, 29, 193-208 (1977).

3. Love, T. J., Radiative Heat Transfer, Charles E. Merrill Co., Columbus, Ohio 1968.

4. Kobayashi, H., et al., Coal Devolatilization at High Temperature, Sixteenth Symposium (International) on Combustion, pp. 411-426, The Combustion Institute, Pittsburgh, Pa 1977.

5. Field, M. A., et al., Combustion of Pulverized Coal, BCURA, Leatherhead, England, 1967, Edition published by Institute of Fuel, 1974.